On the Spatio-Temporal Analysis and Optimization of AoI in Cell-Free IIoT Networks

Meiyan Song, Hangguan Shan, *Senior Member, IEEE*, Yu Cheng, *Fellow, IEEE*, Weihua Zhuang, *Fellow, IEEE*, Xinyu Li, *Member, IEEE*, Qi Zhang, and Xianhua He

***Abstract*— Cell-free massive multiple-input multiple-output (mMIMO) architecture is a promising solution for Industrial Internet of Things (IIoT) because it not only provides massive connectivity but also eliminates the traditional cell edges. Considering the heterogeneous traffic and requirements in the industry, in this paper, we propose a device priority-aware resource allocation policy under cell-free mMIMO IIoT networks. Specifically, we design a priority-aware frame structure that can be used to provide differentiated age of information (AoI) guarantees for devices of different priorities and locations. To characterize the proposed policy, we develop a general analysis framework to evaluate the signal-to-interference ratio meta distribution and the average AoI of a generic device. The framework captures multiple main features under wireless IIoT networks, including cell-free mMIMO architecture, frame structure, finite-sized geographic areas, densely deployed devices, device priority, retransmission, and interaction among different transmission links. The analytical framework is validated by simulations. Based on the analysis, we study a mean-variance optimization problem to improve the network average AoI, while guaranteeing the average AoI per device. Numerical results show that the proposed frame structure works effectively in enhancing the AoI performance of cell-free IIoT networks.**

***Index Terms*— Industrial Internet of Things, cell-free massive multiple-input multiple-output, frame, age of information.**

Manuscript received 27 July 2023; revised 28 December 2023 and 28 April 2024; accepted 4 August 2024. Date of publication 16 August 2024; date of current version 13 November 2024. This work was supported in part by the National Natural Science Foundation of China under Grant U21B2029 and Grant U21A20456, in part by Zhejiang Provincial Natural Science Foundation of China under Grant LR23F010006, and in part by the Nokia Donation Project. The associate editor coordinating the review of this article and approving it for publication was T. Tsiftsis. *(Corresponding author: Hangguan Shan.)*

Meiyan Song is with the College of Information Engineering, China Jiliang University, Hangzhou 310018, China, and also with the College of Information Science and Electronic Engineering, Zhejiang University, Hangzhou 310027, China (e-mail: songmy@cjlu.edu.cn).

Hangguan Shan is with the College of Information Science and Electronic Engineering, Zhejiang University, Hangzhou 310027, China (e-mail: hshan@zju.edu.cn).

Yu Cheng is with the Department of Electrical and Computer Engineering, Illinois Institute of Technology, Chicago, IL 60616 USA (e-mail: cheng@iit.edu).

Weihua Zhuang is with the Department of Electrical and Computer Engineering, University of Waterloo, Waterloo, ON N2L 3G1, Canada (e-mail: wzhuang@uwaterloo.ca).

Xinyu Li is with the Department of Industrial and Manufacturing Systems Engineering, School of Mechanical Science and Engineering, Huazhong University of Science and Technology, Wuhan 430074, China (e-mail: lixinyu@hust.edu.cn).

Qi Zhang and Xianhua He are with Nokia Solutions and Networks System Technology (Beijing) Company Ltd., Hangzhou 310053, China (e-mail: qi.zhang@nokia-sbell.com; xianhua.he@nokia-sbell.com).

Color versions of one or more figures in this article are available at https://doi.org/10.1109/TWC.2024.3440922.

Digital Object Identifier 10.1109/TWC.2024.3440922

I. Introduction

As a global network infrastructure, the Internet of Things (IoT) enables devices to communicate with each other and realize dynamic information interaction as well as collaborative decision-making [1]. The Industrial Internet of Things (IIoT) focuses on connectivity in industry and thus has some distinctive features. For example, the IIoT networks are built on the traditional industrial infrastructure, so a huge number of devices are densely deployed in a finite-sized geographic area. Further, IIoT applications usually are time and mission-critical with a low tolerance for latency and a high requirement for reliability [2].

Considering the above characteristics, massive multiple-input multiple-output (mMIMO) is suitable for IIoT owing to its ability of massive connectivity and large coverage [3]. However, traditional cellular networks inevitably generate cell boundaries. Cell-edge devices tend to suffer from poor communication quality due to large path loss and interference [4], which defies the requirements of IIoT. To this end, a new architecture named cell-free mMIMO appears promising [5]. The architecture defines a cooperative serving cluster consisting of several spatially adjacent access points (APs) for each device [6]. Then, each device is actually the center of its serving cluster and the conventional cell edges are eradicated. It is demonstrated in [3], [7], [8], and [9] that applying cell-free mMIMO to IIoT networks can lead to further advantages potentially, e.g., improving capacity and data transmission rate.

Despite these benefits, there are many challenges to apply cell-free mMIMO in IIoT networks due to the following reasons. First, there are usually multiple devices coexisting in IIoT, serving various applications such as performance monitoring and intelligent inspection [10]. These devices have heterogeneous traffic characteristics and quality of service (QoS) requirements. Coordinating the resource allocation among multiple applications is necessary but is often not a focus in existing works (e.g., [11], [12], [13]). Second, the correlation between device location and performance has not been fully explored. In a large-scale network, the locations of nodes (APs or devices) are usually modeled as homogeneous Poisson point processes (PPPs), and the performance statistics are independent of the test location [14]. Nevertheless, the assumption is not well-suited for IIoT as the network is usually finite. Nodes at different locations possess different service clusters and suffer from different levels of interference. Evaluating device performance accurately and providing

QoS guarantees for devices at different locations is a major challenge.

In addition to the above two aspects, the existing studies on cell-free mMIMO IIoT networks mainly focus on capacity enhancement [3], [7], [8], [9]. It is inadequate in terms of the stringent requirements for real-time information in IIoT networks. From this perspective, age of information (AoI) is an appropriate metric [15], [16]. Specifically, AoI measures the time elapsed since the last successfully received packet at the destination was generated at the source [17], [18]. From the perspective of receivers, AoI carries a wider connotation than traditional metrics such as latency and throughput, because it contains information on the sampling frequency. For cell-free mMIMO IIoT networks, AoI-aware system design is in a nascent stage.

In this paper, we investigate the application of cell-free mMIMO in IIoT networks and propose a corresponding resource allocation policy to meet the stringent requirements of IIoT applications for real-time information delivery. First, we design a priority-aware frame structure and device grouping strategy to provide differentiated AoI guarantees for devices of different priorities and locations. Then, considering the spatio-temporal characteristics of cell-free mMIMO IIoT networks, we derive mathematical expressions for the location dependent network performance, in terms of the signal-to-interference ratio (SIR) meta distribution and the average AoI of a generic device. Specifically, the locations of devices and APs are modeled as independent binomial point processes (BPPs) [19], and two typical types of sources in IIoT, namely bufferless sources and buffered sources, are studied. By utilizing mean-variance optimization, we further study how to determine the optimal number of groups for each priority. The contributions of this paper are three-fold:

- Taking advantage of the characteristics of cell-free mMIMO architecture, we design a priority-aware frame structure to satisfy differentiated AoI requirements for multiple applications in IIoT networks. By adjusting the number of devices transmitted at the same time, the proposed scheme supports devices of each priority to adjust their own transmission period without affecting other devices. The scheme is flexible and can be well adapted to the dynamically varying network environments.
- We establish an analytical framework for location dependent SIR meta distribution and average AoI in cell-free mMIMO IIoT networks. The framework captures multiple key features under the network of interest, including cell-free mMIMO architecture, frame structure, finite-sized geographic areas, device/AP number, device location, device priority, retransmission, and interference. Further, we study a mean-variance optimization problem to balance the network average AoI and the average AoI of each device.
- We verify the accuracy of our analysis through simulations. Numerical results reveal the relationship between device location and AoI performance. As the distance from the device to the network center increases, the AoI performance of network-interior devices improves slightly, while that of network-edge devices deteriorates severely with the shrink of service clusters. Further, increasing the transmission period can improve the average AoI of a generic device effectively under the networks with heavy traffic.

The remainder of this paper is organized as follows. The related work is reviewed in Section II. In Section III, we detail the spatio-temporal configuration for the cell-free mMIMO IIoT networks and design a priority-aware frame structure. Section IV is focused on the evaluation of the SIR meta distribution and the average AoI. In Section V, we study the mean-variance optimization problem to improve the network average AoI while guaranteeing average AoI per device. The simulation and numerical results are presented in Section VI to demonstrate the accuracy of the analysis and the effectiveness of the frame structure design, followed by conclusions in Section VII.

II. Related Work

In this section, we review related studies on cell-free architecture, medium access control (MAC) protocol, AoI metric in IIoT networks, and finite-sized wireless network performance analysis. Cell-free architecture has been introduced to IIoT networks [3], [7], [8], [9]. Peng et al. investigate pilot and power allocation [7], demonstrating that cell-free mMIMO is superior to centralized mMIMO in terms of average weighted sum rate. Then, they derive lower bounds of downlink ergodic rate under different precoding schemes such as full-pilot zero-forcing, local zero-forcing, and maximum-ratio transmission [8]. Pilot power and transmission power are jointly optimized there to improve the weighted sum rate. By leveraging dual deep deterministic policy gradient, Liu et al. develop a random access and power allocation strategy to improve the data transmission rate under cell-free mMIMO IIoT networks [9]. Taking random data arrivals into account, Wang et al. obtain a closed-form expression of the capacity under cell-free mMIMO IIoT networks, based on which the power control coefficients are determined [3].

Considering densely deployed devices, an effective MAC protocol is important in IIoT networks. Gao et al. propose a new MAC protocol for IIoT networks [2], utilizing mini-slot based carrier sensing, synchronization carrier sensing, differentiated assignment cycles, and superimposed mini-slot assignment. The protocol tries to avoid packet collision and can provide differentiated QoS for devices of different priorities. Based on this MAC protocol, the authors further design a centralized scheduling algorithm based on deep neural network [10]. Also tailored for the device priority in IIoT, an instantaneous channel state information (CSI)-based dynamic joint block length and shared-pilot length algorithm is proposed by Cao et al. [20], where throughput, latency, and signaling overhead are evaluated. To support real-time data flows for IIoT networks, a medium access strategy for long range (LoRa) is proposed by Leonardi et al. [21].

AoI-related work in IIoT networks is summarized as follows. Existing studies focus on the trade-off between AoI and other metrics such as energy consumption [11], [22] and reliability [12], [13]. In [11], Hsu et al. consider energy

consumption when sensors transmit data to the controller, and propose a federated learning-based optimization framework to optimize data sampling. The long-term data transmission energy consumption is minimized there while maintaining information freshness. In [12], Chan et al. study a joint packet encoding policy to reduce packet error rate while safeguarding AoI. Considering the harsh communication environment in the industrial field, Wang et al. obtain the average AoI under the packet loss and present an optimal communication strategy consisting of the data updating rate and code length [23]. In addition to the unreliable transmission, the influence of data processing on AoI is evaluated by Li et al. [24], where edge computing can be introduced to offload data and reduce AoI. In [25], Xiong et al. propose a predict-compare transmission scheme to reduce the average AoI for short packet transmission in IIoT.

Different from the study of infinite wireless networks, performance analysis in finite-sized wireless networks is usually very challenging since the interference depends on the node locations. To address this issue, references [26], [27], [28] focus on the networks with specific shapes, while authors of [29] and [30] consider arbitrarily shaped networks. With the circular network assumption, Parida et al. model the user and AP locations as independent BPPs and derive the user rate coverage for cell-free mMIMO systems with finite capacity fronthaul links [26], while Ernest et al. analyze the outage probability and AoI for multi-access edge computing-enabled IIoT networks [27]. In [29], Guo et al. analyze outage performance by utilizing moment generating function-based framework and reference link power gain-based framework. In [30], Tong et al. obtain the distribution of the distance between two uniformly distributed nodes in arbitrarily shaped networks.

Compared with the existing studies, the main contributions of this work lie in two aspects. i) The proposed priority-aware frame structure can coordinate the transmissions of devices with heterogeneous traffic, satisfying differentiated AoI requirements in IIoT networks. Further, the design takes advantage of the cell-free mMIMO architecture, and thus can significantly improve the transmission success probability even if a large number of devices are required to transmit simultaneously. ii) The analytical framework of the average AoI captures the impact of temporal variability of the traffic, spatial irregularity of node locations, and interdependency between node performance and location. The research results can guide us on how to balance the network average AoI and the average AoI of each device.

III. System Model

In this section, we first present the network topology, channel model, and traffic model for the proposed cell-free mMIMO IIoT network. Then, a frame structure is designed for devices of different priorities. Finally, we introduce the concept of average AoI of a generic device. The main notations are summarized in Table I.

TABLE I
Summary of Notation

Notation	Definition
$a^{\mathrm{s}}_{0\,\vert\hat{\Phi}_{\mathbf{x}_0}}$	Conditional active probability of device $\mathbf{x}_0$ for source type s given spatial realization $\hat{\Phi}_{\mathbf{x}_0}$
$A^{\mathrm{s}}_v(t)$	AoI of the device at location $(v,0)$ for source type s and time slot t
$\overline{A}^{\mathrm{s}}_v$	Average AoI of the device at location $(v,0)$ for source type s
$\overline{A}^{\mathrm{s}}_{v\,\vert\hat{\Phi}_{\mathbf{x}_0}}$	Average AoI of the device at location $(v,0)$ for source type s given spatial realization $\hat{\Phi}_{\mathbf{x}_0}$
C	Number of time slots within a frame
$\mathcal{D}(\mathbf{o},R_{\mathrm{d}})$	Disk centered at the origin and of radius R_{d}
$f^{\mathrm{s}}_v(\vartheta)$	PDF of the non-zero conditional transmission success probability for the device at location $(v,0)$ given s
$F^{\mathrm{s}}_v(\vartheta)$	CDF of the conditional transmission success probability for the device at location $(v,0)$ given s
g_c	Number of groups for devices of priority c
h_{i0}	Channel gain between device $\mathbf{x}_i$ and AP $\mathbf{y}_0$
k	Number of APs associated by one device
l_{i0}	Pathloss function between device $\mathbf{x}_i$ and AP $\mathbf{y}_0$
M	Number of antennas equipped by an AP
N_{a}, $N_{\mathrm{d},c}$	Number of APs and devices of priority c
R_{a}, R_{d}	Radius of association region and IIoT networks
$\mathrm{s}\in\{\mathrm{bl},\mathrm{bd}\}$	Bufferless sources or buffered sources
α	path loss exponent
Φ_{a}, $\Phi_{\mathrm{d},c}$	Binomial point process modeling the locations of APs and devices of priority c
$\Phi^{\mathbf{x}_0}_{\mathrm{d}}$	Binomial point process modeling the locations of devices belonging to the same group as $\mathbf{x}_0$
$\sigma^{\mathrm{s}}_{i,t}$	Indicator representing whether device $\mathbf{x}_i$ is transmitting packets at time t given source type s
θ	SIR threshold for successful transmissions
ξ_c	Packet arrival probability in a slot for devices of priority c
ϖ_c	Risk aversion index for devices of priority c
$\gamma^{\mathrm{s}}_{00,t\,\vert\hat{\Phi}_{\mathbf{x}_0}}$	Conditional outage probability of the link between device $\mathbf{x}_0$ and AP $\mathbf{y}_0$ at time t given $\hat{\Phi}_{\mathbf{x}_0}$ and s
$\gamma^{\mathrm{s}}_{0n\,\vert\hat{\Phi}_{\mathbf{x}_0}}$	Conditional outage probability of the link between device $\mathbf{x}_0$ and AP $\mathbf{y}_0$ given $\hat{\Phi}_{\mathbf{x}_0}$ and s
$\mu^{\mathrm{s},k}_{0\,\vert\hat{\Phi}_{\mathbf{x}_0}}$	Conditional transmission success probability of device $\mathbf{x}_0$ given $\hat{\Phi}_{\mathbf{x}_0}$, s, and the number of associated APs k
$\mu^{\mathrm{s}}_{0\,\vert\hat{\Phi}_{\mathbf{x}_0}}$	Conditional transmission success probability of device $\mathbf{x}_0$ given $\hat{\Phi}_{\mathbf{x}_0}$ and s

A. Network Model

We focus on an uplink cell-free mMIMO IIoT network. The network is deployed in a finite-sized geographic area $\mathcal{A}\subset\mathbb{R}^2$. For expositional simplicity, consider $\mathcal{A}=\mathcal{D}(\mathbf{o},R_{\mathrm{d}})$, where $\mathcal{D}(\mathbf{o},R_{\mathrm{d}})$ represents a disk centered at the origin and of radius R_{d}.[1] The network has N_{a} APs, each equipped with M antennas for maximal ratio combining (MRC) reception. The AP locations follow a uniform BPP, Φ_{a}. All these APs are connected to a central processing unit (CPU) through reliable fronthaul links. There are a large number of single-antenna devices such as sensors densely deployed in this area. These devices are categorized into C types according to their priority. Without loss of generality, we assume that priority c_1 is higher than priority c_2 if $c_1<c_2$, where $\{c_1,c_2\}\subseteq\{1,2,\ldots,C\}$. The number of devices of priority c is denoted by $N_{\mathrm{d},c}$ and their locations follow a BPP, $\Phi_{\mathrm{d},c}$, where $c\in\{1,2,\ldots,C\}$. All devices transmit with the same power. As shown in Fig. 1, in the user-centric cell-free mMIMO, each device is served simultaneously by the set of APs within a distance of R_{a} to the device. Without loss of generality, we assume that R_{a} is smaller than R_{d}.

[1]For analysis tractability, we use the circular network assumption as in [26], [27], and [28]. It is worth noting that our model can be extended to analyze networks of other shapes, e.g., square and rectangular.

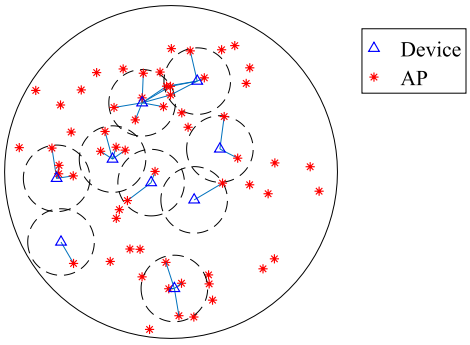

Fig. 1. An illustration of the cell-free mMIMO IIoT networks.

B. Channel Model

In this subsection, we introduce the channel model. The channel between any device and AP is subjected to path loss and small-scale fading. In the singular path loss model, $r^{-\alpha}$ is used to represent the path loss with propagation distance r and path loss exponent α. However, this unbounded model does not apply to the cell-free mMIMO networks since the APs and devices can be arbitrarily close [31]. Thus, we consider a non-singular path loss function, $l(r) = [\max\{R_0, r\}]^{-\alpha}$, where R_0 is the reference distance [14]. To ensure analysis tractability, we assume that the small-scale fading follows Rayleigh fading with unit mean [32], which varies independently and identically distributed across different links and time.[2]

C. Traffic Model

We consider a time-slotted system, with equal-length time slots. In the uplink, devices and their associated APs are source nodes and destination nodes, respectively. For devices, the generation as well as sending of packets occur at the boundary of time slots. The transmission of each packet consumes a full time slot. For a device of priority c, its packet generation follows a Bernoulli process. At the beginning of each time slot, the device can generate a packet with probability ξ_c, $c \in \{1, 2, \ldots, C\}$. Note that the packet arrival probability can represent the status updating rate at sources. Two types of sources are considered:

1) Bufferless Sources: Bufferless sources have no buffer to store packets. Upon generating a packet, the source will drop it directly or discard it after sending, which depends on whether the transmission is allowed at the current time slot.

2) Buffered Sources: Each buffered source has a unit-size buffer and the newly generated packet will substitute for the old one, if any. A source with a non-empty buffer will send its packet to the destination when the transmission is permitted. Unlike the bufferless sources, a buffered source keeps the sent packet in its buffer until it is successfully transmitted or a new packet is generated. As such, these queueing activities satisfy last-come-first-served protocol with replacement (LCFS-R).

Remark 1: Various applications in the IIoT networks can be divided into two types. One type requires only the latest information from the source nodes. Once the latest packet is successfully delivered, the old one will be useless. Typical examples are the monitoring services for temperature, pressure, and inventory. In the other type, every packet should be transmitted, such as in control services for automated operations. The bufferless sources and buffered sources under consideration are suitable for the first type of applications. Using the infinite buffer model and considering the first-come-first-served (FCFS) protocol, this work can be extended to study the second type of applications [34], [35].

[2]Note that the proposed analytical framework can be extended to analyze other fading such as Nakagami-*m* [33].

D. Priority-Aware Frame Structure and Device Grouping

Considering the heterogeneous AoI requirements of various devices in IIoT networks, in this subsection we design a priority-aware frame structure to realize effective resource allocation among devices of different priorities. As illustrated in Fig. 2, a frame consists of C time slots. In particular, the c-th time slot of each frame belongs to the devices of priority c. Further, devices in IIoT networks are often densely deployed, which can incur severe crosstalk. Hence, we divide all devices of priority c into g_c groups. Each group utilizes the same time slot for transmission, and g_c groups transmit in different frames in turn. The period of devices of priority c is $g_c C$ slots. In general, the number of devices with a higher priority is smaller [2], i.e., $N_{\mathrm{d},c_1} < N_{\mathrm{d},c_2}$ if $c_1 < c_2$. As a result, the period allocated to devices of a higher priority can be shorter to provide differentiated QoS for all devices in the network.

To facilitate time slot allocation according to the proposed priority-aware frame structure, the network controller needs to collect the priority information on all the devices and decides grouping strategy, i.e., find the optimal g_c for each priority. In Section V, we are to study the optimization of g_c, with the aim of improving the network average performance while providing the information freshness guarantee for each device. Then, the network controller is in charge of broadcasting the grouping results and each device randomly occupies one of the allocated time slots accordingly. Prioritizing and grouping are preempted and remain unchanged in subsequent communications. If the quantity of devices of a certain priority changes, the network controller adjusts and broadcasts grouping configuration for them. It is worth noting that in this case the transmissions of other devices are not affected. Therefore, the proposed priority-aware frame structure has low implementation complexity. In addition, to achieve synchronization in cell-free mMIMO IIoT networks, specifically designed synchronization protocols such as the broadcasting-based cooperative time synchronization protocol [36] can be utilized.

Remark 2: Compared with the existing IIoT MAC protocols such as [2] and [10], the proposed frame structure is targeted at cell-free mMIMO, where one device can be served by multiple APs and an MRC receiver is equipped in each AP. Therefore, the impact of packet collisions is reduced and multiple devices can transmit simultaneously.

E. Performance Metrics

Different from the large-scale networks, where locations of nodes are usually modeled as homogeneous PPP and the

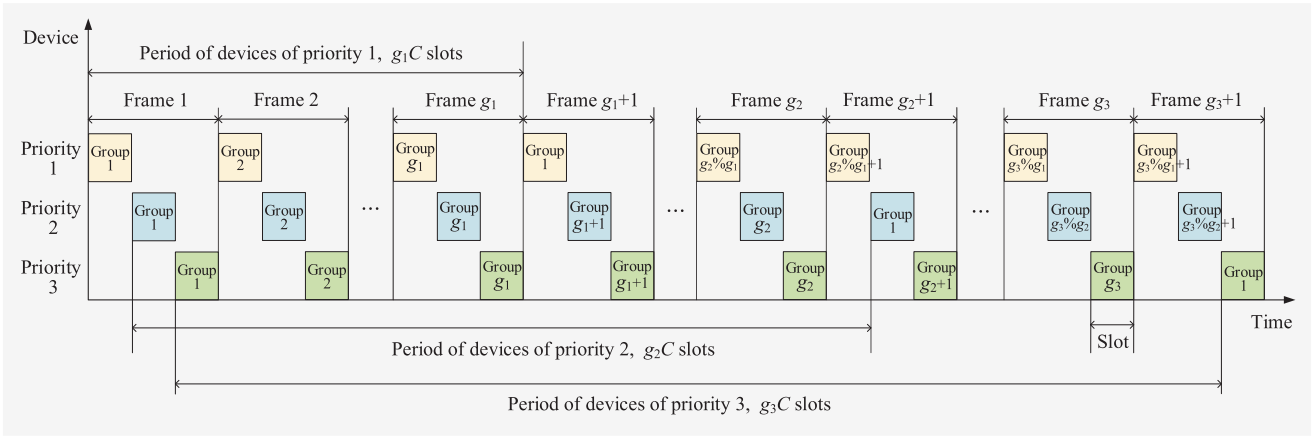

Fig. 2. An illustration of the priority-aware frame structure and device grouping given $C = 3$, where % denotes the remainder operation.

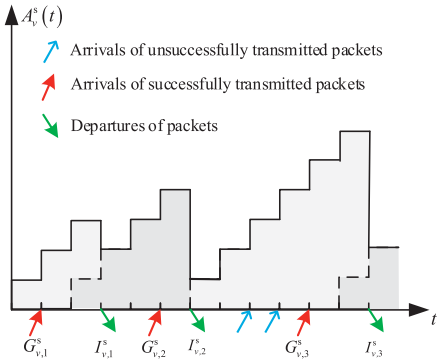

Fig. 3. The evolution curve of AoI of the reference device at location $\mathbf{x}_0 = (v, 0)$. $A_v^{\mathrm{s}}(t)$ is the value of AoI at the beginning of slot t. The solid lines in the figure represent the AoI of $\mathbf{x}_0$, while the dotted lines represent the age of the packet that is transmitting.

performance of a typical node can be used to represent that of a generic node, a finite-sized IIoT network has location-dependent performance.[3] Here, we focus on the reference device at location $\mathbf{x}_0 = (v, 0)$, which can represent any device in the network by rotating the coordinate axes or resizing v. For the convenience of notation, we utilize the same variable to describe one node and its location. Next, we give the definition of AoI of device $\mathbf{x}_0$.

In the time-slotted system, the device at location $\mathbf{x}_0 = (v, 0)$ transmits packets to its associated APs, which is then forwarded to the CPU. The time for the second phase can be ignored when utilizing reliable fronthaul links [37]. The AoI of device $\mathbf{x}_0$ at time slot t is defined as

$$A_v^{\mathrm{s}}(t) = t - G_{v,\kappa_t^*}^{\mathrm{s}}, \tag{1}$$

where $\kappa_t^* = \arg\max_{\kappa} \left\{ G_{v,\kappa}^{\mathrm{s}} \middle| I_{v,\kappa}^{\mathrm{s}} < t \right\}$ is the index of the latest received packet by the CPU till time t, $G_{v,\kappa}^{\mathrm{s}}$ and $I_{v,\kappa}^{\mathrm{s}}$ are the time slots when the κ-th successfully received packet is generated and received, respectively. Superscript $\mathrm{s} \in \{\mathrm{bl}, \mathrm{bd}\}$ indicates the bufferless sources or buffered sources.

Fig. 3 illustrates the evolution curve of AoI of device $\mathbf{x}_0$. The AoI adds one at the beginning of each slot unless the CPU receives a new packet at the last time slot. Assuming that the AoI remains constant within a time slot, the average AoI of the reference device at location $\mathbf{x}_0 = (v, 0)$ is defined as $\overline{A}_v^{\mathrm{s}} = \limsup_{T\to\infty} \frac{1}{T} \sum_{t=1}^{T} A_v^{\mathrm{s}}(t)$ [22].

[3]Due to the circular network assumption, location dependent performance here implies that the network performance is specific to the distance from the origin to the node of interest.

IV. Performance Analysis

In this section, we evaluate the AoI performance in the IIoT network considering that the proposed cell-free mMIMO architecture and priority-aware frame structure are employed. Specifically, we first derive the conditional transmission success probability of the reference device $\mathbf{x}_0$. Then, we obtain the analytical expression of the conditional average AoI of $\mathbf{x}_0$. Finally, based on all the aforementioned analyses, we arrive at the SIR meta distribution and the average AoI of $\mathbf{x}_0$.

A. Conditional Transmission Success Probability

Consider that the reference device $\mathbf{x}_0$ is of priority c and in an interference-limited regime with negligible background noise [38]. At time slot t, if $\mathbf{x}_0$ is sending out a packet, the received SIR at its associated AP, $\mathbf{y}_0$, can be written as

$$\mathrm{SIR}_{00,t}^{\mathrm{s}} = \frac{\hat{h}_{00} l\left(\|\mathbf{x}_0 - \mathbf{y}_0\|\right)}{\sum_{\mathbf{x}_i \in \Phi_{\mathrm{d}}^{\mathbf{x}_0} \setminus \{\mathbf{x}_0\}} \sigma_{i,t}^{\mathrm{s}} h_{i0} l\left(\|\mathbf{x}_i - \mathbf{y}_0\|\right)}, \tag{2}$$

where $\hat{h}_{00}$ following the Gamma distribution $\mathrm{Ga}(M, 1)$ denotes the total received channel gain at AP $\mathbf{y}_0$ from device $\mathbf{x}_0$ after MRC reception process [38], h_{i0} following the exponential distribution $\mathrm{Exp}(1)$ models the independent channel gain for the interfering device $\mathbf{x}_i$ [39], $\Phi_{\mathrm{d}}^{\mathbf{x}_0}$ represents the devices of the same priority and belonging to the same group as $\mathbf{x}_0$, $\sigma_{i,t}^{\mathrm{s}}$ is an indicator representing whether device $\mathbf{x}_i$ is transmitting packets at time t (in this case, $\sigma_{i,t}^{\mathrm{s}} = 1$) or not (in this case, $\sigma_{i,t}^{\mathrm{s}} = 0$), and $l\left(\|\mathbf{x}_i - \mathbf{y}_0\|\right)$ is the non-singular path loss function between device $\mathbf{x}_i$ and AP $\mathbf{y}_0$. In the following, we abbreviate $l\left(\|\mathbf{x}_i - \mathbf{y}_0\|\right)$ as l_{i0} for symbolic simplicity. The transmission is unsuccessful if the SIR at AP $\mathbf{y}_0$ is smaller than a decoding threshold θ. As such, given the spatial realization $\hat{\Phi}_{\mathbf{x}_0} = \Phi_{\mathrm{a}} \cup \Phi_{\mathrm{d}}^{\mathbf{x}_0}$, the conditional outage probability of the link between device $\mathbf{x}_0$ and AP $\mathbf{y}_0$ at time t can be defined as

$$\gamma_{00,t\,|\hat{\Phi}_{\mathbf{x}_0}}^{\mathrm{s}} = \mathbb{P}\left(\mathrm{SIR}_{00,t}^{\mathrm{s}} < \theta \middle| \hat{\Phi}_{\mathbf{x}_0}\right). \tag{3}$$

For bufferless sources, there is no correlation among different slots as retransmission is not allowed. For buffered sources, however, the conditional outage probability of different slots is correlated, which complicates the subsequent analysis. To this end, we introduce the men-field approximation [40], i.e., we assume that each queue at a buffered source node observes the time-averages of the activity indicators of other queues but evolves independently of their current state. It is noteworthy that here we utilize the mean-field approximation in the temporal domain. While the approximation allows us to decouple the evolution of queues over time, the transmissions at individual links remain mutually dependent in space due to the interactions caused by interference. With this assumption, transmissions of a buffered source node can be regarded as independent over time with an outage probability $\gamma^{\mathrm{bd}}_{00\,|\hat{\Phi}_{\mathbf{x}_0}} = \lim_{t\to\infty} \gamma^{\mathrm{bd}}_{00,t\,|\hat{\Phi}_{\mathbf{x}_0}}$. For completeness, let $\gamma^{\mathrm{bl}}_{00\,|\hat{\Phi}_{\mathbf{x}_0}} = \gamma^{\mathrm{bl}}_{00,t\,|\hat{\Phi}_{\mathbf{x}_0}}$. To derive the conditional outage probability, we need to average out the fading terms in (2).

Theorem 1: Consider the reference device of priority c at location $\mathbf{x}_0 = (v, 0)$. Given spatial realization $\hat{\Phi}_{\mathbf{x}_0}$, the conditional outage probability of the link between $\mathbf{x}_0$ and its associated AP $\mathbf{y}_0$ is given by

$$\gamma^{\mathrm{s}}_{00\,|\hat{\Phi}_{\mathbf{x}_0}} \approx \sum_{k_1=0}^{M} \binom{M}{k_1} (-1)^{k_1} \prod_{\mathbf{x}_i \in \Phi_{\mathrm{d}}^{\mathbf{x}_0} \setminus \{\mathbf{x}_0\}} \left[1 - \frac{a^{\mathrm{s}}_{i\,|\hat{\Phi}_{\mathbf{x}_0}}}{1 + l_{00}/(\beta l_{i0})}\right], \quad (4)$$

where $\beta = \theta k_1 (M!)^{-\frac{1}{M}}$, and $a^{\mathrm{s}}_{i\,|\hat{\Phi}_{\mathbf{x}_0}} = \lim_{t\to\infty} \mathbb{P}(\sigma^{\mathrm{s}}_{i,t} = 1 \mid \hat{\Phi}_{\mathbf{x}_0})$ is the conditional active probability of device $\mathbf{x}_i$ in the steady state.

Proof: Please see Appendix A. ∎

In the cell-free mMIMO network, all APs are connected to the CPU via reliable fronthaul links. Therefore, it is sufficient if at least one of the APs, connected to the device, can successfully receive the packet.[4] As such, given the spatial realization $\hat{\Phi}_{\mathbf{x}_0}$, the conditional transmission success probability of the reference device associating with k ($\in \{0, 1, \ldots, N_{\mathrm{a}}\}$) APs is $\mu^{\mathrm{s},k}_{0\,|\hat{\Phi}_{\mathbf{x}_0}} = 1 - \prod_{n=0}^{k-1} \gamma^{\mathrm{s}}_{0n\,|\hat{\Phi}_{\mathbf{x}_0}}$. Averaging out k, the conditional transmission success probability of device $\mathbf{x}_0$ is given by

$$\mu^{\mathrm{s}}_{0\,|\hat{\Phi}_{\mathbf{x}_0}} = \sum\nolimits_{k=1}^{N_{\mathrm{a}}} \chi(k) \mu^{\mathrm{s},k}_{0\,|\hat{\Phi}_{\mathbf{x}_0}}, \quad (5)$$

where $\chi(k)$ is the probability that one device is associated with k APs. According to the definition of BPP, $\chi(k)$ can be written as

$$\chi(k) = \begin{cases} \chi_1(k), & 0 \le v \le R_{\mathrm{d}} - R_{\mathrm{a}} \\ \chi_2(k), & R_{\mathrm{d}} - R_{\mathrm{a}} < v \le R_{\mathrm{d}} + R_{\mathrm{a}}, \end{cases} \quad (6)$$

where $\chi_1(k) = \binom{N_{\mathrm{a}}}{k} \left(\frac{R_{\mathrm{a}}^2}{R_{\mathrm{d}}^2}\right)^k \left(1 - \frac{R_{\mathrm{a}}^2}{R_{\mathrm{d}}^2}\right)^{N_{\mathrm{a}}-k}$, $\chi_2(k) = \binom{N_{\mathrm{a}}}{k} \left(\frac{S}{\pi R_{\mathrm{d}}^2}\right)^k \left(1 - \frac{S}{\pi R_{\mathrm{d}}^2}\right)^{N_{\mathrm{a}}-k}$, and $S = R_{\mathrm{a}}^2 (\phi_1 - \frac{1}{2}\sin 2\phi_1) + R_{\mathrm{d}}^2 (\phi_2 - \frac{1}{2}\sin 2\phi_2)$ with $\phi_1 = \arccos\left(\frac{v^2 + R_{\mathrm{a}}^2 - R_{\mathrm{d}}^2}{2vR_{\mathrm{a}}}\right)$ and $\phi_2 = \arccos\left(\frac{v^2 + R_{\mathrm{d}}^2 - R_{\mathrm{a}}^2}{2vR_{\mathrm{d}}}\right)$ is the area of the association region of $\mathbf{x}_0$ given $R_{\mathrm{d}} - R_{\mathrm{a}} < v \le R_{\mathrm{d}} + R_{\mathrm{a}}$. The derivation of S will be given in Section IV-C.

Similarly, we can obtain the conditional transmission success probability for a generic device $\mathbf{x}_i$. Next, we consider the conditional active probability $a^{\mathrm{s}}_{i\,|\hat{\Phi}_{\mathbf{x}_0}}$ in Theorem 1 by utilizing the queueing theory.

Theorem 2: Consider that the device $\mathbf{x}_i$ is of the same priority and belongs to the same group as device $\mathbf{x}_0$. Given its conditional transmission success probability $\mu^{\mathrm{s}}_{i\,|\hat{\Phi}_{\mathbf{x}_0}}$, if the devices in the IIoT network operate as bufferless sources and buffered sources, the conditional active probability of $\mathbf{x}_i$ can be respectively written as

$$a^{\mathrm{bl}}_{i\,|\hat{\Phi}_{\mathbf{x}_0}} = \xi_c, \quad (7a)$$

$$a^{\mathrm{bd}}_{i\,|\hat{\Phi}_{\mathbf{x}_0}} = \frac{1 - (1 - \xi_c)^{g_c C}}{1 - (1 - \mu^{\mathrm{bd}}_{i\,|\hat{\Phi}_{\mathbf{x}_0}})(1 - \xi_c)^{g_c C}}. \quad (7b)$$

Proof: For bufferless sources, the conditional active probability is equal to the packet arrival probability in a slot. For buffered sources, we can solve it by leveraging the queueing theory. Let Ξ_0 (Ξ_1) denote the probability that the buffer is empty (non-empty) when device $\mathbf{x}_i$ is permitted to transmit. Then, we have

$$\begin{cases} \Xi_0 \left[1 - (1 - \xi_c)^{g_c C}\right] = \Xi_1 \mu^{\mathrm{bd}}_{i\,|\hat{\Phi}_{\mathbf{x}_0}} (1 - \xi_c)^{g_c C} \\ \Xi_0 + \Xi_1 = 1. \end{cases} \quad (8)$$

Solving it yields Ξ_1, i.e., the conditional active probability of $\mathbf{x}_i$. ∎

B. Conditional Average AoI

In this subsection, we calculate the conditional average AoI of $\mathbf{x}_0$ given its conditional transmission success probability obtained in the last subsection.

Theorem 3: Consider the reference device of priority c at location $\mathbf{x}_0 = (v, 0)$. Given the conditional transmission success probability $\mu^{\mathrm{s}}_{0\,|\hat{\Phi}_{\mathbf{x}_0}}$, if the devices in the IIoT network operate as bufferless sources and buffered sources, the conditional average AoI of $\mathbf{x}_0$ can be respectively written as

$$\overline{A}^{\mathrm{bl}}_{v\,|\hat{\Phi}_{\mathbf{x}_0}} = \frac{g_c C}{\xi_c \mu^{\mathrm{bl}}_{0\,|\hat{\Phi}_{\mathbf{x}_0}}} - \frac{g_c C}{2} + \frac{1}{2}, \quad (9)$$

$$\overline{A}^{\mathrm{bd}}_{v\,|\hat{\Phi}_{\mathbf{x}_0}} = \frac{g_c C}{\mu^{\mathrm{bd}}_{0\,|\hat{\Phi}_{\mathbf{x}_0}}} + \frac{1}{\xi_c} - \frac{g_c C + 1}{2}. \quad (10)$$

Proof: Taking buffered sources as an example. Let us analyze reference device $\mathbf{x}_0$ with conditional transmission success probability $\mu^{\mathrm{bd}}_{0\,|\hat{\Phi}_{\mathbf{x}_0}}$. Consider an arbitrary time slot after one attempted transmission and denote it as the $\hbar$-th time slot. We assume that the corresponding AoI of this slot is $p + qT_c$, where $p \in \{1, 2, \ldots, T_c\}$, $q \in \{0, 1, \ldots, \infty\}$, and $T_c = g_c C$ is the transmission period. Then, we can draw the

[4]Note that other complex detection techniques (e.g., centralized detection [41]) are promising options at the cost of larger backhaul traffic and implementation complexity. However, to ensure analysis tractability and unveil design insight, similar to [38] we assume that, as long as one of the associated APs can successfully receive data from that device, the transmission from the device to the CPU is successful. The study in [41] shows that the spectral efficiency of this case can be better than the case that the CPU uniformly combines signals preprocessed by APs due to the reduced impact of APs over a badly interfered channel.

conclusion that at least one of the $q+1$ transmissions before the current time slot must have been successful. We mark these $q+1$ transmissions as the 1st, 2nd, …, and $(q+1)$-th attempt, respectively. Consider three cases as follows:

Case 1: q = 0. The packet arriving at time slot $\hbar - p$ is successfully delivered at time slot $\hbar - 1$. The probability of this case is

$$\Delta(p,0) = \xi_c(1-\xi_c)^{p-1}\mu^{\mathrm{bd}}_{0\,|\hat{\Phi}_{\mathbf{x}_0}}. \tag{11}$$

Case 2: $q \neq 0$ and the $(q+1)$-th attempt is successful. There were $(qT_c + p - 1)$ time slots with no packet arrivals and the first q transmissions have failed. The probability of this case is

$$\Delta(p,q) = \xi_c(1-\xi_c)^{qT_c+p-1}(1-\mu^{\mathrm{bd}}_{0\,|\hat{\Phi}_{\mathbf{x}_0}})^q\mu^{\mathrm{bd}}_{0\,|\hat{\Phi}_{\mathbf{x}_0}}. \tag{12}$$

Case 3: $q \neq 0$ and the $(\ell+1)$-th attempt is successful, $\ell \in \{0,1,\ldots,q-1\}$. Similarly, the probability of this case is

$$\begin{aligned}&\Delta(p,\ell)\\ &= \xi_c(1-\xi_c)^{\ell T_c+p-1}(1-\mu^{\mathrm{bd}}_{0\,|\hat{\Phi}_{\mathbf{x}_0}})^{\ell}\mu^{\mathrm{bd}}_{0\,|\hat{\Phi}_{\mathbf{x}_0}} \times \Big\{(1-\xi_c)^{(q-\ell)T_c}\\ &+ \sum_{i=0}^{q-\ell-1}\left\{\left[1-(1-\xi_c)^{T_c}\right](1-\xi_c)^{iT_c}\left(1-\mu^{\mathrm{bd}}_{0\,|\hat{\Phi}_{\mathbf{x}_0}}\right)^{q-\ell-i}\right\}\Big\}.\end{aligned} \tag{13}$$

Here, $(1-\xi_c)^{(q-\ell)T_c}$ represents that no packets arrived after the $(\ell+1)$-th attempt, and $\left[1-(1-\xi_c)^{T_c}\right](1-\xi_c)^{iT_c}\left(1-\mu^{\mathrm{bd}}_{0\,|\hat{\Phi}_{\mathbf{x}_0}}\right)^{q-\ell-i}$ represents that one packet arrived between the $(\ell+i+1)$-th attempt and $(\ell+i+2)$-th attempt, but was not transmitted successfully in the next $(q-\ell-i)$ attempts.

Aggregating (11)-(13), we can obtain the conditional average AoI of $\mathbf{x}_0$ at the next time slot after each attempted transmission transmission, denoted by $\tilde{A}^{\mathrm{bd}}_{v\,|\hat{\Phi}_{\mathbf{x}_0}}$, as follows

$$\begin{aligned}&\tilde{A}^{\mathrm{bd}}_{v\,|\hat{\Phi}_{\mathbf{x}_0}}\\ &= \sum_{p=1}^{T_c} p\Delta(p,0) + \sum_{q=1}^{\infty}\sum_{p=1}^{T_c}(p+qT_c)\left[\Delta(p,q) + \sum_{\ell=0}^{q-1}\Delta(p,q)\right]\\ &= \left(\frac{1}{\mu^{\mathrm{bd}}_{0\,|\hat{\Phi}_{\mathbf{x}_0}}} - 1\right)T_c + \frac{1}{\xi_c}.\end{aligned} \tag{14}$$

Then, the conditional average AoI of $\mathbf{x}_0$ can be written as

$$\overline{A}^{\mathrm{bd}}_{v\,|\hat{\Phi}_{\mathbf{x}_0}} = \frac{\tilde{A}^{\mathrm{bd}}_{v\,|\hat{\Phi}_{\mathbf{x}_0}} + (\tilde{A}^{\mathrm{bd}}_{v\,|\hat{\Phi}_{\mathbf{x}_0}} + T_c - 1)}{2} = \tilde{A}^{\mathrm{bd}}_{v\,|\hat{\Phi}_{\mathbf{x}_0}} + \frac{T_c}{2} - \frac{1}{2}. \tag{15}$$

Substituting (14) into (15) yields (10). As for bufferless sources, there is no retransmission and the successful delivery of one packet must occur in the same time slot as the generation of the packet. The derivation process is similar to buffered sources. To avoid redundancy, the detail is omitted.[5] ■

[5]Theorem 3 can also be proved by expanding Theorem 3 in [42], considering the relationship between the inter-generation and service time.

From the above theorem, increasing the number of groups g_c has two opposite effects on the AoI performance. On one hand, a large g_c increases the transmission period of devices and hinders information updating. Ignoring the effect of other factors, i.e., given ξ_c and $\mu^{\mathrm{s}}_{0\,|\hat{\Phi}_{\mathbf{x}_0}}$, $\overline{A}^{\mathrm{s}}_{v\,|\hat{\Phi}_{\mathbf{x}_0}}$ is positively correlated with g_c. On the other hand, a large g_c decreases the number of devices transmitting at the same time slot, increasing the transmission success probability. So, $\mu^{\mathrm{s}}_{0\,|\hat{\Phi}_{\mathbf{x}_0}}$ and g_c are positively correlated. The two effects jointly determine the conditional average AoI of $\mathbf{x}_0$. Therefore, there exists an optimal g_c value that maximizes the AoI performance.

C. SIR Meta Distribution and Average AoI

According to the analysis in the previous subsection, the conditional transmission success probability and the AoI performance are closely related. So, in this subsection, we are first concerned about the cumulative distribution function (CDF) of the conditional transmission success probability, which is commonly known as the SIR meta distribution. For the reference device at location $\mathbf{x}_0 = (v,0)$, the SIR meta distribution is defined as

$$F^{\mathrm{s}}_v(\vartheta) = \mathbb{P}\left(\mu^{\mathrm{s}}_{0\,|\hat{\Phi}_{\mathbf{x}_0}} < \vartheta\right). \tag{16}$$

It is noteworthy that the SIR meta distribution here is different from [43], which focuses on large-scale networks. Given the locations of nodes modeled by PPP, the SIR meta distribution allows one to obtain information about the proportion of users whose transmission success probabilities exceed a certain threshold. In this work, we consider the finite-sized IIoT networks, where the SIR meta distribution captures the performance specific to the distance to the network center across different realizations.

To derive the SIR meta distribution, we start with two key distance distributions: One is the distribution of the distance from the reference device to its associated APs, and the other is the distribution of the distance from the reference AP to interfering devices.

Lemma 1: Consider the reference device at location $\mathbf{x}_0 = (v,0)$. Given the association radius R_{a}, the distance from $\mathbf{x}_0$ to a generic associated AP, R, has the following distribution

$$f_R(r|v) = \begin{cases} f_{R,1}(r|v), & 0 \le v \le R_{\mathrm{d}} - R_{\mathrm{a}} \\ f_{R,2}(r|v), & R_{\mathrm{d}} - R_{\mathrm{a}} < v \le R_{\mathrm{d}}, \end{cases} \tag{17}$$

where

$$f_{R,1}(r|v) = \frac{2r}{R_{\mathrm{a}}^2},\ 0 \le r \le R_{\mathrm{a}}, \tag{18}$$

$$f_{R,2}(r|v) = \begin{cases} \dfrac{2\pi r}{S}, & 0 \le r \le R_{\mathrm{d}} - v \\ \dfrac{2r}{S}\phi_3, & R_{\mathrm{d}} - v < r \le R_{\mathrm{a}}, \end{cases} \tag{19}$$

with $\phi_3 = \arccos\left(\frac{v^2+r^2-R_{\mathrm{d}}^2}{2vr}\right)$.

Proof: Please see Appendix B. ■

Lemma 2: Consider the reference AP at location $\mathbf{y}_u = (u,0)$. The distance from $\mathbf{y}_u$ to a generic device, W, has the

following distribution

$$f_W(w|u)=\begin{cases} f_{W,1}(w|u), & 0\le w\le R_{\rm d}-u \\ f_{W,2}(w|u), & R_{\rm d}-u<w\le R_{\rm d}+u, \end{cases} \tag{20}$$

where $f_{W,1}(w|u)=\frac{2w}{R_{\rm d}^2}$ *and* $f_{W,2}(w|u)=\frac{2w}{\pi R_{\rm d}^2}\arccos\left(\frac{u^2+w^2-R_{\rm d}^2}{2uw}\right)$.

Proof: Given the location of the reference AP rather than that of the reference device, Lemma 2 can be obtained using the method for proving Lemma 1. To avoid redundancy, the specific derivation is omitted. ∎

It is worth noting that due to the location independence of devices and APs, the distances from device $\mathbf{x}_0$ to any of its associated APs follow the same distribution. Armed with Theorems 1-2 and Lemmas 1-2, we can derive the SIR meta distribution of bufferless sources and buffered sources.

Theorem 4: Consider the reference device of priority c at location $\mathbf{x}_0=(v,0)$. If the devices in the IIoT network operate as bufferless sources, the CDF of its conditional transmission success probability is given by

$$F_v^{\rm bl}(\vartheta)=\chi(0)+\sum\nolimits_{k=1}^{N_{\rm a}}\chi(k)F_{v,k}^{\rm bl}(\vartheta), \tag{21}$$

in which

$$F_{v,k}^{\rm bl}(\vartheta)\approx\frac{1}{2}-\int_0^\infty {\rm Im}\left\{\vartheta^{-j\rho}\sum_{k_2=0}^{j\rho}\binom{j\rho}{k_2}(-1)^{k_2}\times\left[\sum_{\substack{v_{k_1}\ge 0\\ v_0+\ldots+v_M=k_2}}\mathcal{U}(v_{k_1})\mathcal{V}(\mathcal{Z})\right]^k\right\}\frac{d\rho}{\pi\rho}, \tag{22}$$

$$\mathcal{U}(v_{k_1})=\Omega_{v_M}^{k_2}\left[\prod_{0\le k_1\le M}\binom{M}{k_1}^{v_{k_1}}(-1)^{k_1v_{k_1}}\right], \tag{23}$$

$$\mathcal{V}_1(\mathcal{Z})=\int_0^{R_{\rm a}}\left[\int_0^{R_{\rm d}+v}\mathcal{Z}f_W(w|v)dw\right]^{\frac{N_{{\rm d},c}}{g_c}-1}f_R(r|v)dr, \tag{24}$$

with $j=\sqrt{-1}$, $\mathcal{Z}=\prod_{0\le k_1\le M}\left\{1-\frac{\xi_c}{1+l(r)/[\beta l(w)]}\right\}^{v_{k_1}}$, $\Omega_{v_M}^{k_2}=\frac{(k_2)!}{v_0!v_1!\ldots v_M!}$, *and* ${\rm Im}\{\cdot\}$ *representing the imaginary part of a complex quantity.*

Proof: Please see Appendix C. ∎

For analytical tractability, when proving Theorem 4, we utilize an approximation to evaluate the interference suffered by AP $\mathbf{y}_n$ to which device $\mathbf{x}_0$ is associated. Simulation results in Section VI validate the approximation under different network parameters.

Theorem 5: Consider the reference device of priority c at location $\mathbf{x}_0=(v,0)$. If the devices in the IIoT network operate as buffered sources, the CDF of its conditional transmission success probability is given by

$$F_v^{\rm bd}(\vartheta)=\chi(0)+\sum\nolimits_{k=1}^{N_{\rm a}}\chi(k)F_{v,k}^{\rm bd}(\vartheta), \tag{25}$$

in which

$$F_{v,k}^{\rm bd}(\vartheta)\approx\frac{1}{2}-\int_0^\infty {\rm Im}\left\{\vartheta^{-j\rho}\sum_{k_2=0}^{j\rho}\binom{j\rho}{k_2}(-1)^{k_2}\times\left[\sum_{\substack{v_{k_1}\ge 0\\ v_0+\ldots+v_M=k_2}}\mathcal{U}(v_{k_1})\mathcal{K}(\mathcal{H})\right]^k\right\}\frac{d\rho}{\pi\rho}, \tag{26}$$

$$\mathcal{K}(\mathcal{H})=\int_0^{R_{\rm a}}\left[\int_0^{R_{\rm d}}\int_0^{2\pi}\mathcal{H}\frac{z}{\pi {R_{\rm d}}^2}d\phi dz\right]^{\frac{N_{{\rm d},c}}{g_c}-1}f_R(r|v)dr, \tag{27}$$

and $\mathcal{H}$ *is given as (28), shown at the bottom of the next page, with* $w_0=\left(\left|z^2+v^2+2zv\cos\phi\right|\right)^{\frac{1}{2}}$. *The results of the buffered sources can be obtained iteratively as* $F_v^{\rm bd}(\vartheta)=\chi(0)+\lim_{t\to\infty}\sum_{k=1}^{N_{\rm a}}\chi(k)F_{v,k,t}^{\rm bd}(\vartheta)$. *Particularly, at the initial stage ($t=0$), we have* $F_{v,k,0}^{\rm bd}(\vartheta)=F_{v,k}^{\rm bl}(\vartheta)$.

Proof: Please see Appendix D. ∎

Note that the conditional average AoI of $\mathbf{x}_0$ approaches infinity when the number of associated APs is 0. The corresponding probability is $\chi(0)$. Therefore, we calculate the CDF of the non-zero conditional transmission success probability for bufferless sources and buffered sources as

$$\tilde{F}_v^{\rm s}(\vartheta)=\sum\nolimits_{k=1}^{N_{\rm a}}\frac{\chi(k)}{1-\chi(0)}F_{v,k}^{\rm s}(\vartheta). \tag{29}$$

For buffered sources, the calculation of $\tilde{F}_v^{\rm bd}(\vartheta)$ is performed iteratively as indicated in Theorem 5. Further, all the moments of the conditional transmission success probability are necessary, leading to complex calculations. With the conditional transmission success probability bounded between 0 and 1, a more efficient way is to approximate the desired distribution by leveraging the Beta distribution [44]. Then, we have the following theorem.

Theorem 6: The probability density function (PDF) of the non-zero conditional transmission success probability can be approximated as

$$f_v^{\rm s}(\vartheta)=\lim_{t\to\infty}f_{v,t}^{\rm s}(\vartheta)=\lim_{t\to\infty}\frac{\vartheta^{\gamma_{v,t}^{\rm s}-1}(1-\vartheta)^{\beta_{v,t}^{\rm s}-1}}{B\left(\gamma_{v,t}^{\rm s},\beta_{v,t}^{\rm s}\right)}, \tag{30}$$

where $B(\cdot)$ *is the Beta function,* $\gamma_{v,t}^{\rm s}$ *and* $\beta_{v,t}^{\rm s}$ *are given by*

$$\gamma_{v,t}^{\rm s}=\frac{m_{v,{\rm s},t}^{(1)}\beta_{v,t}^{\rm s}}{1-m_{v,{\rm s},t}^{(1)}},\ \beta_{v,t}^{\rm s}=\frac{\left[1-m_{v,{\rm s},t}^{(1)}\right]\left[m_{v,{\rm s},t}^{(1)}-m_{v,{\rm s},t}^{(2)}\right]}{m_{v,{\rm s},t}^{(2)}-\left[m_{v,{\rm s},t}^{(1)}\right]^2}, \tag{31}$$

with $m_{v,{\rm s},t}^{(b)}$ *given by*

$$m_{v,{\rm bl},t}^{(b)}\approx\sum_{k=1}^{N_{\rm a}}\sum_{k_2=0}^{b}\frac{\chi(k)}{1-\chi(0)}\binom{b}{k_2}(-1)^{k_2}\times\left[\sum_{\substack{v_{k_1}\ge 0\\ v_0+\ldots+v_M=k_2}}\mathcal{U}(v_{k_1})\mathcal{V}(\mathcal{Z})\right]^k, \tag{32}$$

$$m_{v,{\rm bd},t}^{(b)}\approx\sum_{k=1}^{N_{\rm a}}\sum_{k_2=0}^{b}\frac{\chi(k)}{1-\chi(0)}\binom{b}{k_2}(-1)^{k_2}$$

$$\times \left[\sum_{\substack{v_{k_1} \geq 0 \\ v_0 + \ldots + v_M = k_2}} \mathcal{U}(v_{k_1}) \mathcal{K}(\mathcal{H}) \right]^k. \quad (33)$$

Proof: Similar to [43], we can approximate the distribution of the conditional transmission success probability by utilizing the Beta distribution with the same mean and variance. ∎

Finally, by substituting (30) in Theorem 6 into (9) and (10) in Theorem 3, we can evaluate the average AoI for $\mathbf{x}_0$, given by

$$\overline{A}_v^{\mathrm{bl}} = \int_0^1 \frac{g_c C}{\xi_c \vartheta} f_v^{\mathrm{bl}}(\vartheta) d\vartheta - \frac{g_c C}{2} + \frac{1}{2}, \quad (34)$$

$$\overline{A}_v^{\mathrm{bd}} = \int_0^1 \frac{g_c C}{\vartheta} f_v^{\mathrm{bd}}(\vartheta) d\vartheta + \frac{1}{\xi_c} - \frac{g_c C + 1}{2}. \quad (35)$$

Equations (34) and (35) quantify the average information freshness of device $\mathbf{x}_0$ over a long period of time when the devices in the IIoT network operate as bufferless sources and buffered sources, respectively. The expressions take into account the effects of multiple key factors in the wireless network, including cell-free mMIMO architecture, frame structure, queuing dynamics, device location, retransmission, and interference.

V. Optimization of AoI

In this section, we study how to determine the number of groups g_c to stimulate the advantages of the proposed priority-aware frame structure under cell-free mMIMO architecture. Take the devices of priority c as an example since the parameter settings of devices of different priorities are decoupled. We refer to the mean of the average AoI of all the devices of priority c in the IIoT network as the network average AoI. To improve the network average AoI of devices of priority c while providing the information freshness guarantee for each device, we consider the following mean-variance optimization (MVO) problem [45]:

$$\min_{g_c} \quad \mathbb{E}[\overline{A}_v^{\mathrm{s}}] + \varpi_c \mathbb{D}[\overline{A}_v^{\mathrm{s}}], \quad (36a)$$

$$\text{s.t.} \quad \mathrm{g_c} \in \mathbb{N}_+, \quad (36b)$$

$$0 \leq v \leq R_{\mathrm{d}}, \quad (36c)$$

where $\mathbb{E}[\overline{A}_v^{\mathrm{s}}] = \int_0^{R_{\mathrm{d}}} \overline{A}_v^{\mathrm{s}} \frac{2v}{R_{\mathrm{d}}^2} dv$ is the network average AoI of devices of priority c, $\mathbb{D}[\overline{A}_v^{\mathrm{s}}] = \int_0^{R_{\mathrm{d}}} \left(\overline{A}_v^{\mathrm{s}}\right)^2 \frac{2v}{R_{\mathrm{d}}^2} dv - \mathbb{E}^2[\overline{A}_v^{\mathrm{s}}]$ is the variance of the average AoI of all the devices of priority c, $\mathbb{E}[\overline{A}_{v_q}^{\mathrm{s}}] + \varpi_c \mathbb{D}[\overline{A}_{v_q}^{\mathrm{s}}]$ is the AoI cost, and ϖ_c is the risk aversion index. In the portfolio theory, ϖ_c depends on the investor's individual preferences, reflecting the investor's tolerance for investment risk, and is usually less than ten [45], [46]. In this work, ϖ_c should be appropriately set to balance the network average AoI and the average AoI of each device. We will study the impact of its choice in Section VI-D. Considering that the expression of $\overline{A}_v^{\mathrm{s}}$ is complex and v is a continuous variable on the interval $[0, R_{\mathrm{d}}]$, solving optimization problem (36) directly faces large computational complexity. Therefore, we consider discretizing the problem. Specifically, the whole network region is divided into Q disjoint circles $\{\mathcal{R}_q\}_{q=1}^Q$:

$$\mathcal{R}_q = \mathcal{D}\left(\mathbf{o}, \frac{q}{Q} R_{\mathrm{d}}\right) \setminus \mathcal{D}\left(\mathbf{o}, \frac{q-1}{Q} R_{\mathrm{d}}\right), \quad (37)$$

where $\mathcal{R}_q$ represents the q-th circle. The difference between the inner radius and outer radius of each circle is $\frac{R_{\mathrm{d}}}{Q}$. As such, the first circle is a disk centered at the origin and of radius $\frac{R_{\mathrm{d}}}{Q}$. Next, we choose one point in each circle and use the average AoI of this point to represent the performance of all points in the region. For the point selected in the q-th circle, its distance to the origin is $v_q = \frac{qR_{\mathrm{d}}}{Q}$. As a result, (36) is transformed into:

$$\min_{g_c} \quad \mathbb{E}[\overline{A}_{v_q}^{\mathrm{s}}] + \varpi_c \mathbb{D}[\overline{A}_{v_q}^{\mathrm{s}}], \quad (38a)$$

$$\text{s.t.} \quad \mathrm{g_c} \in \mathbb{N}_+, \quad (38b)$$

$$q \in \{1, 2, \ldots, Q\}, \quad (38c)$$

where $\mathbb{E}[\overline{A}_{v_q}^{\mathrm{s}}] = \sum_{q=1}^Q \overline{A}_{v_q}^{\mathrm{s}} \frac{2q-1}{Q^2}$ and $\mathbb{D}[\overline{A}_{v_q}^{\mathrm{s}}] = \sum_{q=1}^Q (\overline{A}_{v_q}^{\mathrm{s}})^2 \frac{2q-1}{Q^2} - \mathbb{E}^2[\overline{A}_{v_q}^{\mathrm{s}}]$.

According to the analysis at the end of Section 3, increasing g_c has two opposite effects on AoI performance: hindering information updating and improving the transmission success probability. Accordingly, efficient search algorithms such as ternary search [47] can be designed to solve (38).

VI. Simulation and Numerical Results

In this section, we take the reference device of priority c as an example and verify the established mathematical framework through simulations. Then, the effect of different network parameters on the SIR meta distribution and AoI is evaluated. Further, AoI performances of devices at different locations are illustrated. Finally, we study optimization problem (38) to explore the effect of the number of groups g_c on AoI cost. Unless otherwise stated, we adopt the following parameters [19], [38], [40]: $R_{\mathrm{d}} = 30$ m, $R_{\mathrm{a}} = 5$ m, $N_{\mathrm{a}} = 120$, $N_{\mathrm{d},c} = 120$, $g_c = 1$, $C = 3$, $\xi_c = 0.6$, $M = 2$, $\theta = 0$ dB, $\alpha = 4$, and $R_0 = 1$ m. Further, distance v between reference device $\mathbf{x}_0$ and the network center is 5 m without additional description.

A. Validation of the Analyses

Fig. 4 shows the conditional average AoI of the reference device $\mathbf{x}_0$ given the conditional transmission success probability $\mu^{\mathrm{s}}_{0|\hat{\Phi}_{\mathbf{x}_0}}$. Then, the AoI performance here is independent of location v of $\mathbf{x}_0$. The simulation results and numerical

$$\mathcal{H} = \prod_{0 \leq k_1 \leq M} \left[\sum_{k_3=0}^{v_{k_1}} \binom{v_{k_1}}{k_3} (-1)^{k_3} \int_0^{\infty} \frac{(-1)^{k_3} \left[1 - (1-\xi_c)^{g_c C}\right]^{k_3}}{\left[1 - (1-\varsigma)(1-\xi_c)^{g_c C}\right]^{k_3}} dF_z^{\mathrm{bd}}(\varsigma) \left(1 - \frac{1}{1 + \beta l(w_0)/l(r)}\right)^{k_3} \right]. \quad (28)$$

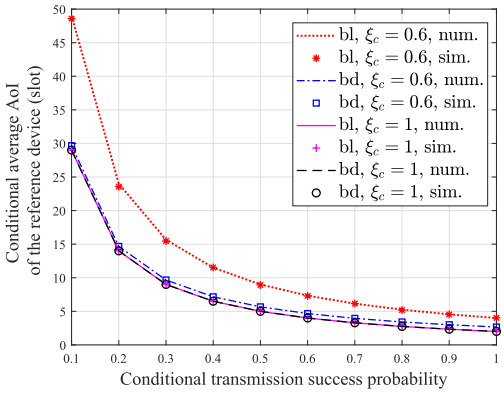

Fig. 4. Conditional average AoI of a specific device under different conditional transmission success probabilities.

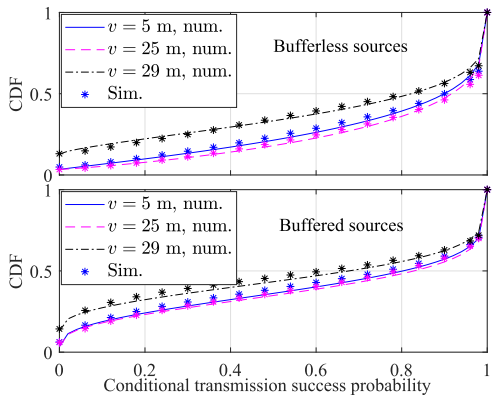

Fig. 5. CDF of the conditional transmission success probability of the reference device at different locations.

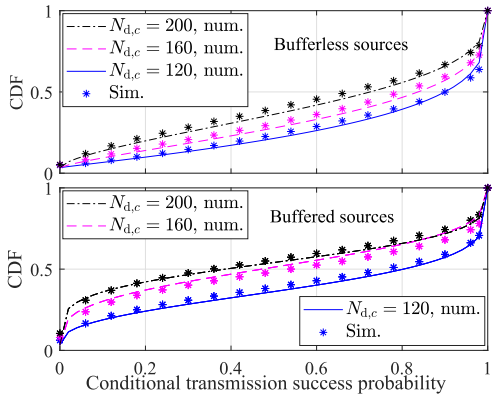

Fig. 6. CDF of the conditional transmission success probability of the reference device under varying number of devices.

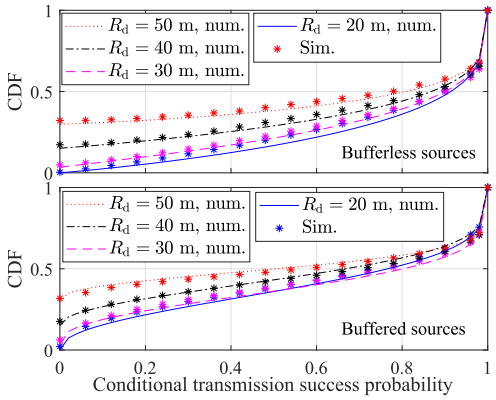

Fig. 7. CDF of the conditional transmission success probability of the reference device under varying network radii.

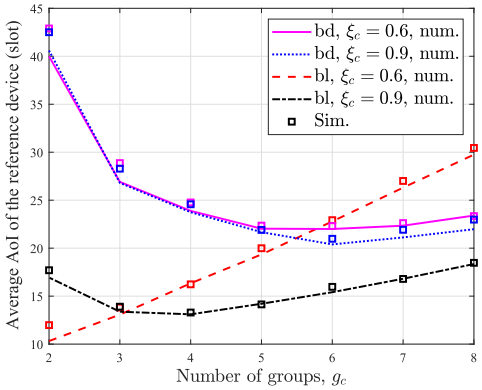

Fig. 8. Effect of the number of groups on the average AoI of the reference device for bufferless sources and buffered sources.

results corresponding to Theorem 3 match well. A small transmission success probability leads to a rapid deterioration in information freshness at destination nodes. Further, given $\xi_c = 1$, the conditional average AoI of $\mathbf{x}_0$ for bufferless sources is the same as that for buffered sources. In this case, the retransmission mechanism does not work and any packets that are not successfully delivered will be replaced by the newly generated packets. Also, the gap of the conditional average AoI between $\xi_c = 0.6$ and 1 for bufferless sources is larger than that for buffered sources, implying that ξ_c generates a larger impact on bufferless sources, consistent with the results derived in (9) and (10).

With respect to Theorems 4-6, Fig. 5 illustrates the CDF of the conditional transmission success probability of reference device $\mathbf{x}_0$ under the varying distances v's between $\mathbf{x}_0$ and the network center. We choose $v = 5$, 25, and 29 m because in the simulations it is observed that the performance with $v \leq 25$ m is very close. The details are presented in Fig. 12. The numerical results and simulation results match well for devices at different locations. At $v = 5$ m, the effect of the number of devices $N_{d,c}$ is shown in Fig. 6. Fig. 7 shows the CDF of the conditional transmission success probability with different network radii R_d's given $v = 5$ m. We observe that the approximation is more suitable for networks with a large radius. In this case, the average distance between one interfering device and device $\mathbf{x}_0$ or its associated APs is larger, and thus the error is small. Another phenomenon is that the probability of transmission success probability being 0 is higher in networks with a larger R_d, because the number of APs (N_a) keeps constant in the simulations. The larger R_d, the lower the density of APs. Then, the serving clusters of devices are more likely to be empty. This inspires us that maintaining a certain AP density is important for the cell-free mMIMO IIoT network.

B. Effect of Different Network Parameters

Fig. 8 and Fig. 9 illustrate the effect of the number of groups (g_c) on the average AoI and non-zero conditional transmission success probability of reference device $\mathbf{x}_0$, respectively. In Fig. 8, in general the average AoI of $\mathbf{x}_0$ decreases first and then grows as g_c increases. This indicates that the negative

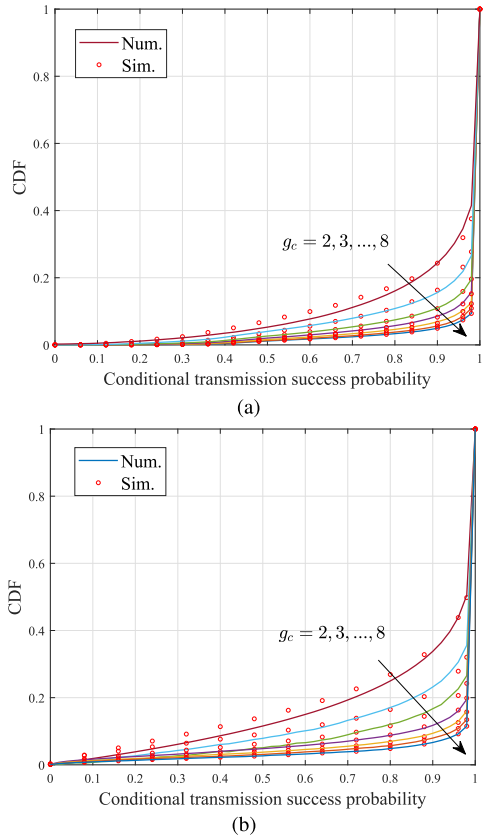

Fig. 9. CDF of the non-zero conditional transmission success probability of the reference device under $\xi_c = 0.6$: (a) Bufferless sources; (b) Buffered sources.

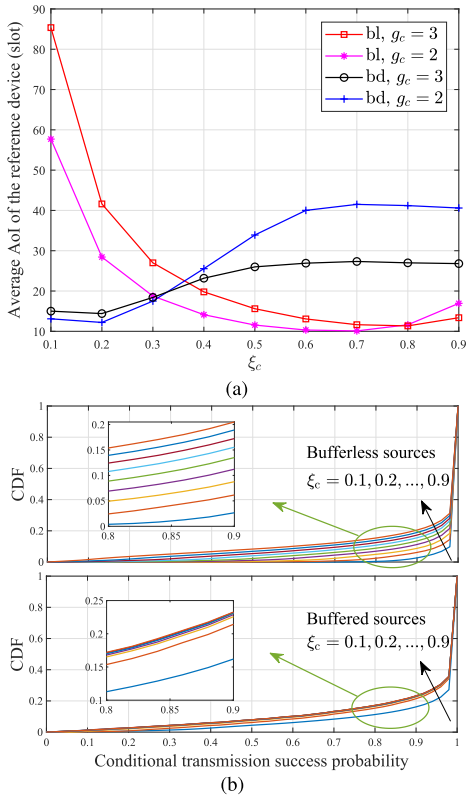

Fig. 10. Effect of the packet arrival probability on the average AoI and conditional transmission success probability of the reference device: (a) Average AoI; (b) CDF of the non-zero conditional transmission success probability under $g_c = 3$.

effect of a larger g_c is to increase the transmission period as well as hinder information updating, and the positive effect is to reduce interference and increase transmission success probability. The observation is consistent with the analysis at the end of Section 3. A special case is bufferless sources with $\xi_c = 0.6$, where the average AoI of $\mathbf{x}_0$ continues to increase. In this case, the positive effect of increasing g_c is not significant due to the light traffic and large conditional transmission success probability. In addition, when the number of groups is large ($g_c \in \{6, 7, 8\}$), the AoI variation of buffered sources is smaller than that of bufferless sources. This is because increasing g_c has a more significant improvement on conditional transmission success probability for buffered sources. This can be observed by comparing Fig. 9(a) with Fig. 9(b). To conclude, the average AoI benefits from increasing the number of groups g_c when the networks operate under heavy traffic.

Fig. 10 shows the impact of the packet arrival probability in a slot ξ_c on the average AoI and non-zero conditional transmission success probability of reference device $\mathbf{x}_0$. To avoid overlapping lines, Fig. 10 and the following figures show only the numerical results. The following observation can be obtained from Fig. 10: 1) Given g_c, the average AoI of $\mathbf{x}_0$ for bufferless sources reduces first and then enlarges as ξ_c increases. This is because, when ξ_c is small, increasing ξ_c leads to more frequent information updating at the destination. However, as ξ_c becomes larger, the network traffic reaches a higher level and the transmissions among different links severely interfere with each other, making the transmissions more prone to failure. 2) For bufferless sources with a larger ξ_c (e.g., $\xi_c \geq 0.8$), increasing g_c is beneficial to improve the average AoI of $\mathbf{x}_0$. However, given small ξ_c, the negative effect of increasing g_c is more profound. This is consistent with the findings in Fig. 8. 3) For buffered sources with $\xi_c \geq 0.6$, the average AoI of $\mathbf{x}_0$ is almost constant. By Theorem 2, $(1 - \xi_c)^{g_c C}$ approximates 0 and the conditional active probability of source nodes approximates 1. Therefore, continuing to increase ξ_c does not cause significant changes in traffic or transmission success probability as shown in Fig. 10(b).

Fig. 11 shows the effect of the number of APs (N_a) and the number of devices of priority c ($N_{\mathrm{d},c}$) on the average AoI of reference device $\mathbf{x}_0$ given $g_c = 2$ and 3. Fig. 11(a) illustrates that the AoI performance improves for both buffered and bufferless sources with the AP number. This is because the more number of APs, the more benefit of cell-free mMIMO architecture. In addition, utilizing buffer can improve the AoI performance given a good communication environment, i.e., the networks with a larger AP density and a larger number of groups. From Fig. 11(b) we can find that the AoI performance deteriorates with the increase in the number of devices, which is more pronounced in the networks with buffered sources because the retransmission causes heavier traffic. Further, this deterioration can be mitigated by appropriately setting g_c.

C. Relationship Between Location and Performance

Fig. 12 gives the average AoI of reference device $\mathbf{x}_0$ under varying SIR threshold θ's and different distances between the

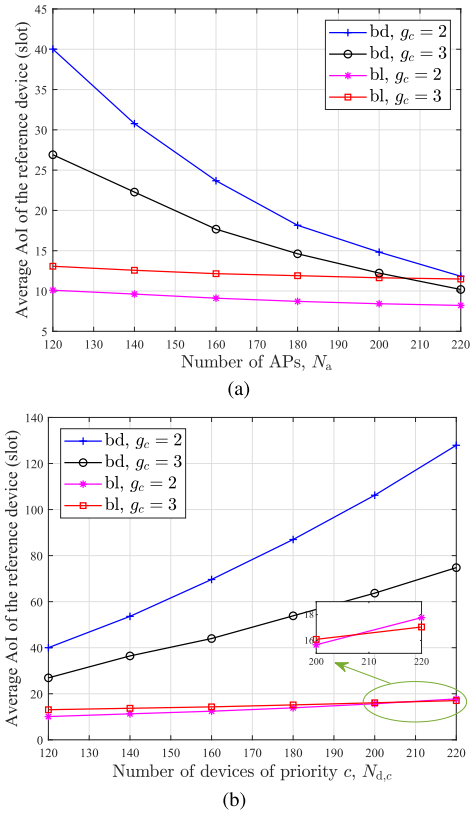

Fig. 11. Effect of the number of nodes on the average AoI of the reference device for bufferless sources and buffered sources: (a) Number of APs; (b) Number of devices of priority c.

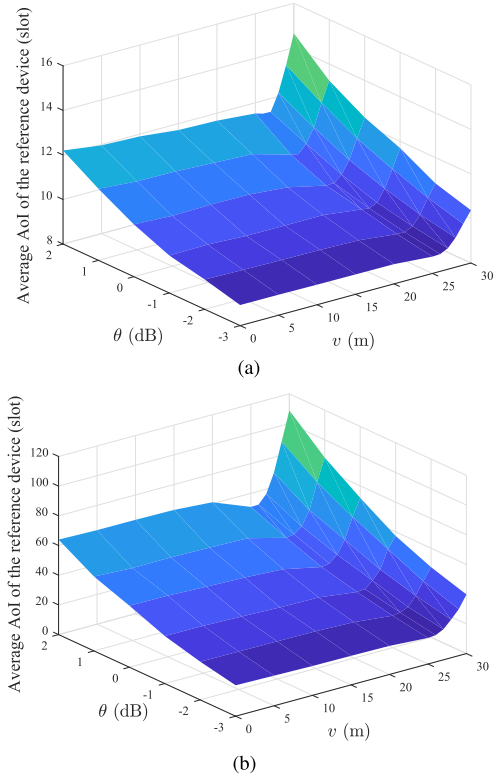

Fig. 12. The average AoI of the reference device under varying SIR threshold θ's and location v's: (a) Bufferless sources; (b) Buffered sources.

device and the network center v's. As v increases, the average AoI of $\mathbf{x}_0$ decreases slowly and then goes up sharply. The minimum value is achieved at $v = 25$ m. Given the network radius $R_d = 30$ m and the association radius $R_a = 25$ m, the distance at which the reference device achieves the best AoI performance is exactly $v = R_d - R_a$. When devices with $v \leq R_d - R_a$, referred to as network-interior devices, are further away from the network center, they are more likely distant from other interfering devices, and thus the less interference they will receive. For devices with $v > R_d - R_a$, referred to as network-edge devices, the area of their association regions decreases rapidly with the increase of v. This suggests that resource allocation can be appropriately skewed toward the edge of the network.

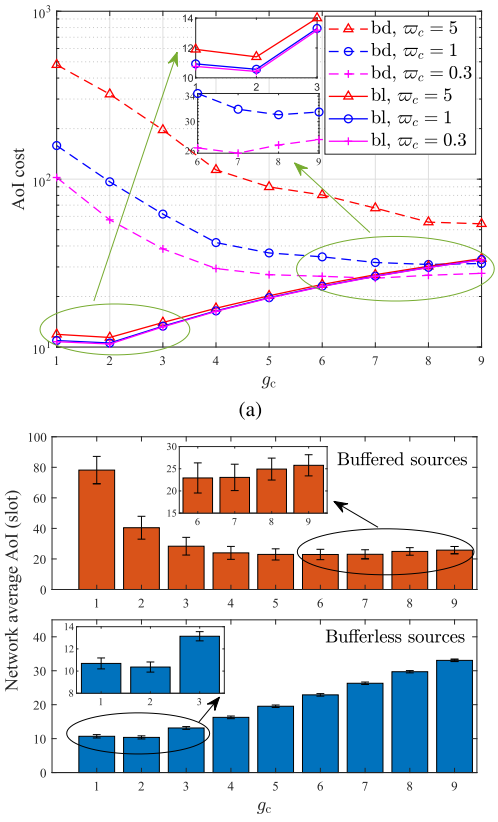

Fig. 13. Effect of the number of groups on the AoI cost and the network average AoI: (a) AoI cost; (b) Network average AoI.

D. Optimization of AoI

Fig. 13(a) shows the solution of optimization problem (38) under different risk aversion indexes ϖ_c's. For the tested parameters, the AoI cost exhibits a convex-like function property with respect to the number of groups g_c,[6] so we can obtain the optimal g_c by ternary search. We observe that the optimal g_c and ϖ_c values are closely related. Given a larger ϖ_c, g_c that results in a more even performance of different devices is more appealing. In addition, for a given ϖ_c value, the optimal number of groups g_c of bufferless sources is significantly smaller than that of buffered sources, as the network with buffered sources has heavier traffic due to retransmission. We can also observe that the value of ϖ_c has a slight effect

[6]Strictly speaking, the AoI cost cannot be called a convex function of g_c because it is not continuous.

on the network with bufferless sources, where the variance of the average AoI of all the devices is small.

To illustrate the effect of g_c on the AoI cost, Fig. 13(b) shows the relationship between the number of groups g_c and the network average AoI of priority c as well as the standard deviation of the average AoI of devices at different locations. It is noteworthy that these results are independent of the setting of ϖ_c. For buffered sources and bufferless sources, the network average AoI decreases first and then increases as g_c increases, which reveals the positive and negative effects of a large g_c and validates the findings from Fig. 8. Further, the standard deviation decreases as g_c increases. This is because the transmission success probability gradually increases and the AoI performance of devices at different locations tends to be consistent.

VII. Conclusion

In this paper, we have explored the feasibility of applying the cell-free mMIMO architecture to IIoT networks, considering the densely deployed devices. We have designed a priority-aware frame structure that can flexibly carry heterogeneous information freshness requirements of multiple applications. The design allows devices of different priorities to adjust their own transmission periods according to their requirements, thus can provide differentiated AoI guarantees. Further, we have proposed a theoretical framework to analyze the SIR meta distribution and average AoI of a generic device. The framework captures the main factors of the IIoT network such as cell-free mMIMO architecture, frame structure, finite-sized geographic areas, device number, device priority, and tangled space-time interactions among links. Based on the analytical model, we have studied a mean-variance optimization problem to balance the network average AoI and average AoI per device. Numerical results show that the performance of network-edge devices is significantly worse than that of network-interior devices, enlightening us that resource can be skewed toward network-edge devices. Increasing the transmission period can enhance the average AoI per device effectively under networks with heavy traffic. In addition, exploring more effective data detection cooperation mode among APs can be considered as a potential direction for future work in cell-free mMIMO IIoT networks. Analysis and design for arbitrarily shaped finite-sized wireless networks require further research.

Appendix A
Sketch of Proof of Theorem 1

According to (3), the conditional outage probability of the link between device $\mathbf{x}_0$ and AP $\mathbf{y}_0$ can be derived as

$$\begin{aligned}
&\mathbb{P}\left(\mathrm{SIR}^{\mathrm{s}}_{00,t} < \theta \middle| \hat{\Phi}_{\mathbf{x}_0}\right)\\
&\overset{(a)}{=} \mathbb{P}\left[\hat{h}_{00} l_{00} < \theta \mathcal{I} \middle| \hat{\Phi}_{\mathbf{x}_0}\right]\\
&\overset{(b)}{=} \mathbb{E}_{\mathcal{I}}\left[1 - \frac{\Gamma\left(M, \theta\mathcal{I}/l_{00}\right)}{\Gamma(M)} \middle| \hat{\Phi}_{\mathbf{x}_0}\right]\\
&\overset{(c)}{\approx} \mathbb{E}_{\mathcal{I}}\left\{\left[1 - \exp\left(-(M!)^{-\frac{1}{M}} \theta\mathcal{I}/l_{00}\right)\right]^M \middle| \hat{\Phi}_{\mathbf{x}_0}\right\}\\
&\overset{(d)}{=} \sum_{k_1=0}^{M} \binom{M}{k_1} (-1)^{k_1} \mathbb{E}\left[\exp\left(-\frac{\beta\theta k_1 \mathcal{I}}{l_{00}}\right) \middle| \hat{\Phi}_{\mathbf{x}_0}\right]\\
&= \sum_{k_1=0}^{M} \binom{M}{k_1} (-1)^{k_1} \prod_{\mathbf{x}_i \in \Phi_{\mathrm{d}}^{\mathbf{x}_0} \setminus \{\mathbf{x}_0\}} \left[1 - \frac{a^{\mathrm{s}}_{i|\hat{\Phi}_{\mathbf{x}_0}}}{1 + l_{00}/(\beta l_{i0})}\right],
\end{aligned} \tag{39}$$

where $\mathcal{I} = \sum_{\mathbf{x}_i \in \Phi_{\mathrm{d}}^{\mathbf{x}_0} \setminus \{\mathbf{x}_0\}} \sigma^{\mathrm{s}}_{i,t} h_{i0} l_{i0}$, $\Gamma(x_1, x_2)$ is the upper incomplete gamma function, and $\beta = \theta k_1 (M!)^{-\frac{1}{M}}$. Step (b) comes from the fact that $\hat{h}_{00} \sim \mathrm{Ga}(M, 1)$ and step (c) holds as $\frac{\Gamma(x_1, x_2)}{\Gamma(x_1)} \approx 1 - [1 - \exp(-x_2 x_3)]^{x_1}$ with $x_3 = (x_1)!^{-\frac{1}{x_1}}$.

Appendix B
Sketch of Proof of Lemma 1

As shown in Fig. 14, we consider three cases.

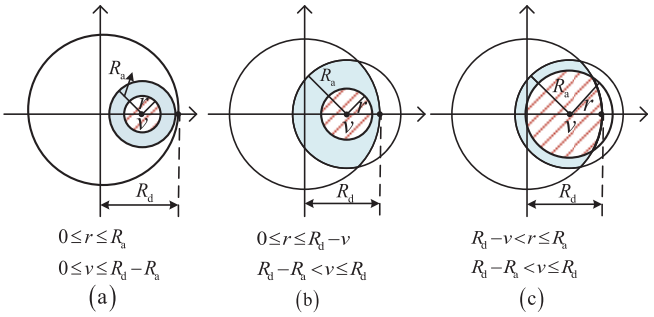

Fig. 14. The relations among the location of $\mathbf{x}_0$, the finite area $\mathcal{A} = \mathcal{D}(\mathbf{o}, R_{\mathrm{d}})$, and the association radius R_{a}.

Case 1: $0 \le v \le R_{\mathrm{d}} - R_{\mathrm{a}}$. In this case, the association region of reference device $\mathbf{x}_0$ is completely contained within the network coverage area. Then, the CDF of the distance from $\mathbf{x}_0$ to a generic associated AP, R, is derived as

$$F_R(r) = \mathbb{P}(R \le r) = \frac{r^2}{R_{\mathrm{a}}^2}, 0 \le r \le R_{\mathrm{a}}. \tag{40}$$

Taking the derivative of $F_R(r)$ with respect to r, we obtain the PDF of R, given by

$$f_R(r) = \frac{2r}{R_{\mathrm{a}}^2}, 0 < r < R_{\mathrm{a}}. \tag{41}$$

Case 2: $R_{\mathrm{d}} - R_{\mathrm{a}} < v \le R_{\mathrm{d}}$ and $0 \le r \le R_{\mathrm{d}} - v$. In this case, the association region of reference device $\mathbf{x}_0$ is the intersection of circle $(x - v)^2 + y^2 = R_{\mathrm{a}}^2$ and circle $x^2 + y^2 = R_{\mathrm{d}}^2$. Then, the abscissa of the intersection of the two circles is $\delta_1 = \frac{v^2 + {R_{\mathrm{d}}}^2 - R_{\mathrm{a}}^2}{2v}$. The area of the intersection is

$$\begin{aligned}
S =& \int_{v - R_{\mathrm{a}}}^{\delta_1} 2\left[R_{\mathrm{a}}^2 - (x - v)^2\right]^{\frac{1}{2}} dx + \int_{\delta_1}^{R_{\mathrm{d}}} 2\left(R_{\mathrm{d}}^2 - x^2\right)^{\frac{1}{2}} dx\\
=& R_{\mathrm{a}}^2 \left(\phi_1 - \frac{1}{2}\sin 2\phi_1\right) + R_{\mathrm{d}}^2 \left(\phi_2 - \frac{1}{2}\sin 2\phi_2\right).
\end{aligned} \tag{42}$$

Then, the PDF of R is $f_R(r) = \frac{2\pi r}{S}$, where $0 \le r \le R_{\mathrm{d}} - v$.

Case 3: $R_{\mathrm{d}} - R_{\mathrm{a}} < v \le R_{\mathrm{d}}$ and $R_{\mathrm{d}} - v < r \le R_{\mathrm{a}}$. Similar to Case 2, the CDF of R can be derived as

$$F_R(r) = \frac{1}{S}\int_{v - r}^{\delta_2} 2\left[r^2 - (x - v)^2\right]^{\frac{1}{2}} dx + \frac{1}{S}\int_{\delta_2}^{R_{\mathrm{d}}} 2\left(R_{\mathrm{d}}^2 - x^2\right)^{\frac{1}{2}} dx$$

$$=\frac{r^2}{S}\left(\phi_3-\frac{1}{2}\sin 2\phi_3\right)+\frac{R_{\rm d}^2}{S}\left(\phi_4-\frac{1}{2}\sin 2\phi_4\right), \quad (43)$$

where $\delta_2=\frac{v^2+R_{\rm d}^2-r^2}{2v}$ and $\phi_4=\arccos\left(\frac{v^2+R_{\rm d}^2-r^2}{2vR_{\rm d}}\right)$. Taking the derivative of $F_R(r)$ with respect to r, we obtain the PDF of R, given by $f_R(r)=\frac{2r}{S}\phi_3$.

Appendix C
Sketch of Proof of Theorem 4

Denote $Y_{0,k,t}^{{\rm s}|\hat{\Phi}_{\mathbf{x}_0}}=1-\prod_{n=0}^{k-1}\gamma_{0n,t\,|\hat{\Phi}_{\mathbf{x}_0}}^{\rm s}$, where t is the index of time slot, and ${\rm s}\in\{{\rm bl},{\rm bd}\}$ represents the type of sources. For bufferless sources, there is no correlation among different slots as retransmission is not allowed. Considering that device $\mathbf{x}_0$ is sending out a packet, the b-th moment of $Y_{0,k,t}^{{\rm bl}|\hat{\Phi}_{\mathbf{x}_0}}$ can be derived as follows:

$$\begin{aligned}
&\mathcal{M}_{Y_{0,k,t}^{{\rm bl}|\hat{\Phi}_{\mathbf{x}_0}}}(b)\\
&=\mathbb{E}\left[\sum\nolimits_{k_2=0}^{b}\binom{b}{k_2}(-1)^{k_2}\left(\prod\nolimits_{n=0}^{k-1}\gamma_{00,t\,|\hat{\Phi}_{\mathbf{x}_0}}^{\rm bl}\right)^{k_2}\right]\\
&=\mathbb{E}\left\{\sum\nolimits_{k_2=0}^{b}\binom{b}{k_2}(-1)^{k_2}\prod\nolimits_{n=0}^{k-1}\left\{\sum\nolimits_{k_1=0}^{M}\binom{M}{k_1}(-1)^{k_1}\right.\right.\\
&\quad\left.\left.\times\prod_{\mathbf{x}_i\in\Phi_{\rm d}^{\mathbf{x}_0}\setminus\{\mathbf{x}_0\}}\left[1-\frac{\xi_c}{1+l_{0n}/(\beta l_{in})}\right]\right\}^{k_2}\right\}\\
&\overset{\rm (a)}{=}\mathbb{E}\left\{\sum_{k_2=0}^{b}\binom{b}{k_2}(-1)^{k_2}\prod_{n=0}^{k-1}\left\{\sum_{\substack{v_{k_1}\geq 0\\ v_0+\ldots+v_M=k_2}}\Omega_{v_M}^{k_2}\prod_{0\leq k_1\leq M}\right.\right.\\
&\quad\left.\left.\times\left\{\binom{M}{k_1}(-1)^{k_1}\prod_{\mathbf{x}_i\in\Phi_{\rm d}^{\mathbf{x}_0}\setminus\{\mathbf{x}_0\}}\left[1-\frac{\xi_c}{1+l_{0n}/(\beta l_{in})}\right]\right\}^{v_{k_1}}\right\}\right\}\\
&=\sum\nolimits_{k_2=0}^{b}\binom{b}{k_2}(-1)^{k_2}\left\{\sum_{\substack{v_{k_1}\geq 0\\ v_0+\ldots+v_M=k_2}}\mathcal{U}(v_{k_1})\right.\\
&\quad\left.\times\mathbb{E}\left\{\prod_{\mathbf{x}_i\in\Phi_{\rm d}^{\mathbf{x}_0}\setminus\{\mathbf{x}_0\}}\prod_{0\leq k_1\leq M}\left[1-\frac{\xi_c}{1+l_{0n}/(\beta l_{in})}\right]^{v_{k_1}}\right\}\right\}^{k}\\
&\overset{\rm (b)}{\approx}\sum_{k_2=0}^{b}\binom{b}{k_2}(-1)^{k_2}\left\{\sum_{\substack{v_{k_1}\geq 0\\ v_0+\ldots+v_M=k_2}}\mathcal{U}(v_{k_1})\int_0^{R_{\rm a}}f_R(r|v)dr\right.\\
&\quad\left.\times\left[\int_0^{R_{\rm d}+v}\prod_{0\leq k_1\leq M}\left[1-\frac{\xi_c}{1+\frac{l(r)}{\beta l(w)}}\right]^{v_{k_1}}f_W(w|v)dw\right]^{\frac{N_{{\rm d},c}}{g_c}-1}\right\}^{k},
\end{aligned} \quad (44)$$

where step (a) is derived from Multinomial Theorem and the approximation in step (b) is due to replacing $l_{in}=l(\|\mathbf{x}_i-\mathbf{y}_n\|)$ with $l(\|\mathbf{x}_i-\mathbf{x}_0\|)$. That is, the distance between interfering device $\mathbf{x}_i$ and AP $\mathbf{y}_n$ is substituted with the distance between $\mathbf{x}_i$ and reference device $\mathbf{x}_0$ served by AP $\mathbf{y}_n$. We take this approximation to simplify the calculation. Specifically, one device may be served by multiple APs in the cell-free mMIMO network. Considering that the association regions of devices vary with locations and may have an irregular shape as shown in Fig. 14, locating each AP leads to extremely complex mathematical representations. Intuitively, this approximation is more suitable for networks with a large radius, where the average distance from the device or its associated APs to the interfering device is larger. The simulation results verify the feasibility of this approximation under different network parameters. According to Gil-Pelaez theorem, the CDF of $Y_{0,k,t}^{{\rm bl}|\hat{\Phi}_{\mathbf{x}_0}}$ is given by

$$F_{v,k,t}^{\rm bl}(\vartheta)=\frac{1}{2}-\int_0^{\infty}\frac{{\rm Im}\left\{\vartheta^{-j\rho}\mathcal{M}_{Y_{0,k,t}^{{\rm bl}|\hat{\Phi}_{\mathbf{x}_0}}}(j\rho)\right\}}{\pi\rho}d\rho. \quad (45)$$

Combining (6) and omitting subscripts t yields Theorem 4.

Appendix D
Sketch of Proof of Theorem 5

In the initial time, i.e., $t=0$, the conditional active probability of all the devices of priority c is ξ_c. As such, the analysis of buffered sources is similar to that of bufferless sources, leading to $\mathcal{M}_{Y_{0,k,0}^{{\rm bd}|\hat{\Phi}_{\mathbf{x}_0}}}(b)=\mathcal{M}_{Y_{0,k,t}^{{\rm bl}|\hat{\Phi}_{\mathbf{x}_0}}}(b)$. In time slot t, the b-th moment of $Y_{0,k,t}^{{\rm bd}|\hat{\Phi}_{\mathbf{x}_0}}$ can be derived iteratively. For ease of exposition, denote $\eta_{z,t}^{\rm bd}=\mathbb{P}(\sigma_{i,t}^{\rm bd}=1\,|\,\|\mathbf{x}_i\|=z)$. Then, we have

$$\begin{aligned}
&\mathcal{M}_{Y_{0,k,t}^{{\rm bd}|\hat{\Phi}_{\mathbf{x}_0}}}(b)\\
&=\sum\nolimits_{k_2=0}^{b}\binom{b}{k_2}(-1)^{k_2}\left\{\sum_{\substack{v_{k_1}\geq 0\\ v_0+\ldots+v_M=k_2}}\mathcal{U}(v_{k_1})\right.\\
&\quad\left.\times\mathbb{E}\left\{\prod_{\mathbf{x}_i\in\Phi_{\rm d}^{\mathbf{x}_0}\setminus\{\mathbf{x}_0\}}\prod_{0\leq k_1\leq M}\left[1-\frac{\mathbb{P}(\sigma_{i,t}^{\rm bd}=1)}{1+l_{0n}/(\beta l_{in})}\right]^{v_{k_1}}\right\}\right\}^{k}\\
&\approx\sum_{k_2=0}^{b}\binom{b}{k_2}(-1)^{k_2}\left\{\sum_{\substack{v_{k_1}\geq 0\\ v_0+\ldots+v_M=k_2}}\mathcal{U}(v_{k_1})\int_0^{R_{\rm a}}\left\{\int_0^{R_{\rm d}}\int_0^{2\pi}\prod_{0\leq k_1\leq M}\right.\right.\\
&\quad\times\left[1-\eta_{z,t}^{\rm bd}\left(1-\frac{1}{1+\beta l[(|z^2+v^2+2zv\cos\phi|)^{\frac{1}{2}}]/l(r)}\right)\right]^{v_{k_1}}\\
&\quad\left.\left.\times\frac{z}{\pi {R_{\rm d}}^2}d\phi dz\right\}^{\frac{N_{{\rm d},c}}{g_c}-1}f_R(r|v)dr\right\}^{k}.
\end{aligned} \quad (46)$$

Similarly, we can obtain $F_{v,k,t}^{\rm bd}(\vartheta)$ by utilizing Gil-Pelaez theorem.

References

[1] T. Qiu, J. Chi, X. Zhou, Z. Ning, M. Atiquzzaman, and D. O. Wu, "Edge computing in Industrial Internet of Things: Architecture, advances and challenges," *IEEE Commun. Surveys Tuts.*, vol. 22, no. 4, pp. 2462–2488, 4th Quart., 2020.

[2] J. Gao, W. Zhuang, M. Li, X. Shen, and X. Li, "MAC for machine-type communications in industrial IoT—Part I: Protocol design and analysis," *IEEE Internet Things J.*, vol. 8, no. 12, pp. 9945–9957, Jun. 2021.

[3] X. Wang and C. Zhai, "Dynamic power control for cell-free industrial Internet of Things with random data arrivals," *IEEE Trans. Ind. Informat.*, vol. 18, no. 6, pp. 4138–4147, Jun. 2022.

[4] M. Song, H. Shan, H. H. Yang, and T. Q. S. Quek, "Joint optimization of fractional frequency reuse and cell clustering for dynamic TDD small cell networks," *IEEE Trans. Wireless Commun.*, vol. 21, no. 1, pp. 398–412, Jan. 2022.

[5] H. Q. Ngo, A. Ashikhmin, H. Yang, E. G. Larsson, and T. L. Marzetta, "Cell-free massive MIMO versus small cells," *IEEE Trans. Wireless Commun.*, vol. 16, no. 3, pp. 1834–1850, Mar. 2017.

[6] H. A. Ammar, R. Adve, S. Shahbazpanahi, G. Boudreau, and K. V. Srinivas, "User-centric cell-free massive MIMO networks: A survey of opportunities, challenges and solutions," *IEEE Commun. Surveys Tuts.*, vol. 24, no. 1, pp. 611–652, 1st Quart., 2022.

[7] Q. Peng, H. Ren, C. Pan, N. Liu, and M. Elkashlan, "Resource allocation for uplink cell-free massive MIMO enabled URLLC in a smart factory," *IEEE Trans. Commun.*, vol. 71, no. 1, pp. 553–568, Jan. 2023.

[8] Q. Peng, H. Ren, C. Pan, N. Liu, and M. Elkashlan, "Resource allocation for cell-free massive MIMO-enabled URLLC downlink systems," *IEEE Trans. Veh. Technol.*, vol. 72, no. 6, pp. 7669–7684, Jun. 2023, doi: 10.1109/TVT.2023.3243571.

[9] X. Liu, H. Zhang, X. Wen, K. Long, J. Wang, and L. Sun, "Primal–dual learning for cross-layer resource management in cell-free massive MIMO IIoT," *IEEE Internet Things J.*, vol. 9, no. 18, pp. 17026–17034, Sep. 2022.

[10] J. Gao, M. Li, W. Zhuang, X. Shen, and X. Li, "MAC for machine-type communications in industrial IoT—Part II: Scheduling and numerical results," *IEEE Internet Things J.*, vol. 8, no. 12, pp. 9958–9969, Jun. 2021.

[11] Y.-L. Hsu, C.-F. Liu, H.-Y. Wei, and M. Bennis, "Optimized data sampling and energy consumption in IIoT: A federated learning approach," *IEEE Trans. Commun.*, vol. 70, no. 12, pp. 7915–7931, Dec. 2022.

[12] T.-T. Chan, H. Pan, and J. Liang, "Age of information with joint packet coding in industrial IoT," *IEEE Wireless Commun. Lett.*, vol. 10, no. 11, pp. 2499–2503, Nov. 2021.

[13] H. Farag, S. M. Ali, and C. Stefanovic, "On the analysis of AoI-reliability tradeoff in heterogeneous IIoT networks," in *Proc. IEEE 33rd Annu. Int. Symp. Pers., Indoor Mobile Radio Commun. (PIMRC)*, Sep. 2022, pp. 1038–1042.

[14] H. ElSawy, E. Hossain, and M. Haenggi, "Stochastic geometry for modeling, analysis, and design of multi-tier and cognitive cellular wireless networks: A survey," *IEEE Commun. Surveys Tuts.*, vol. 15, no. 3, pp. 996–1019, 3rd Quart., 2013.

[15] Z. Chen et al., "Analysis of age of information in dual updating systems," *IEEE Trans. Wireless Commun.*, vol. 22, no. 11, pp. 8003–8019, Nov. 2023.

[16] T. Zhang et al., "AoI and PAoI in the IoT-based multisource status update system: Violation probabilities and optimal arrival rate allocation," *IEEE Internet Things J.*, vol. 10, no. 23, pp. 20617–20632, Dec. 2023.

[17] Y. Sun, I. Kadota, R. Talak, and E. Modiano, *Age of Information: A New Metric for Information Freshness*. San Rafael, CA, USA: Morgan & Claypool, 2019.

[18] C. Xu, H. H. Yang, X. Wang, and T. Q. S. Quek, "Optimizing information freshness in computing-enabled IoT networks," *IEEE Internet Things J.*, vol. 7, no. 2, pp. 971–985, Feb. 2020.

[19] M. Afshang and H. S. Dhillon, "Fundamentals of modeling finite wireless networks using binomial point process," *IEEE Trans. Wireless Commun.*, vol. 16, no. 5, pp. 3355–3370, May 2017.

[20] J. Cao, X. Zhu, Y. Jiang, Y. Liu, and F.-C. Zheng, "Short frame structure optimization for industrial IoT with heterogeneous traffic and shared pilot," in *Proc. IEEE Global Commun. Conf. (GLOBECOM)*, Dec. 2020, pp. 1–6.

[21] L. Leonardi, F. Battaglia, and L. Lo Bello, "RT-LoRa: A medium access strategy to support real-time flows over LoRa-based networks for industrial IoT applications," *IEEE Internet Things J.*, vol. 6, no. 6, pp. 10812–10823, Dec. 2019.

[22] B. Zhou and W. Saad, "Joint status sampling and updating for minimizing age of information in the Internet of Things," *IEEE Trans. Commun.*, vol. 67, no. 11, pp. 7468–7482, Nov. 2019.

[23] X. Wang, C. Chen, J. He, S. Zhu, and X. Guan, "AoI-aware control and communication co-design for industrial IoT systems," *IEEE Internet Things J.*, vol. 8, no. 10, pp. 8464–8473, May 2021.

[24] J. Li, J. Tang, and Z. Liu, "On the data freshness for industrial Internet of Things with mobile-edge computing," *IEEE Internet Things J.*, vol. 9, no. 15, pp. 13542–13554, Aug. 2022.

[25] Q. Xiong, X. Zhu, Y. Jiang, J. Cao, X. Xiong, and H. Wang, "Status prediction and data aggregation for AoI-oriented short-packet transmission in industrial IoT," *IEEE Trans. Commun.*, vol. 71, no. 1, pp. 611–625, Jan. 2023.

[26] P. Parida and H. S. Dhillon, "Cell-free massive MIMO with finite fronthaul capacity: A stochastic geometry perspective," *IEEE Trans. Wireless Commun.*, vol. 22, no. 3, pp. 1555–1572, Mar. 2023.

[27] T. Z. H. Ernest and A. S. Madhukumar, "Age of information outage probability analysis for computation offloading in IIoT networks," *IEEE Commun. Lett.*, vol. 27, no. 9, pp. 2471–2475, Sep. 2023.

[28] P. Zhang, I. Nevat, G. W. Peters, G. Xiao, and H.-P. Tan, "Event detection in wireless sensor networks in random spatial sensors deployments," *IEEE Trans. Signal Process.*, vol. 63, no. 22, pp. 6122–6135, Nov. 2015.

[29] J. Guo, S. Durrani, and X. Zhou, "Outage probability in arbitrarily-shaped finite wireless networks," *IEEE Trans. Commun.*, vol. 62, no. 2, pp. 699–712, Feb. 2014.

[30] F. Tong and J. Pan, "Random-to-random nodal distance distributions in finite wireless networks," *IEEE Trans. Veh. Technol.*, vol. 66, no. 11, pp. 10070–10083, Nov. 2017.

[31] Z. Chen and E. Björnson, "Channel hardening and favorable propagation in cell-free massive MIMO with stochastic geometry," *IEEE Trans. Commun.*, vol. 66, no. 11, pp. 5205–5219, Nov. 2018.

[32] S. Kurma, P. K. Sharma, K. Singh, S. Mumtaz, and C.-P. Li, "URLLC-based cooperative industrial IoT networks with nonlinear energy harvesting," *IEEE Trans. Ind. Informat.*, vol. 19, no. 2, pp. 2078–2088, Feb. 2023.

[33] J. Park, J. Choi, and N. Lee, "A tractable approach to coverage analysis in downlink satellite networks," *IEEE Trans. Wireless Commun.*, vol. 22, no. 2, pp. 793–807, Feb. 2023.

[34] W. Lin, L. Li, J. Yuan, Z. Han, M. Juntti, and T. Matsumoto, "Age-of-information in first-come-first-served wireless communications: Upper bound and performance optimization," *IEEE Trans. Veh. Technol.*, vol. 71, no. 9, pp. 9501–9515, Sep. 2022.

[35] A. Kosta, N. Pappas, A. Ephremides, and V. Angelakis, "The age of information in a discrete time queue: Stationary distribution and non-linear age mean analysis," *IEEE J. Sel. Areas Commun.*, vol. 39, no. 5, pp. 1352–1364, May 2021.

[36] B. Li, X. Zhu, Y. Jiang, H. Zeng, and Y. Wang, "Cooperative time synchronization and parameter estimation via broadcasting for cell-free massive MIMO networks," in *Proc. IEEE Wireless Commun. Netw. Conf. (WCNC)*, Apr. 2022, pp. 2100–2105.

[37] A. Papazafeiropoulos, P. Kourtessis, M. D. Renzo, S. Chatzinotas, and J. M. Senior, "Performance analysis of cell-free massive MIMO systems: A stochastic geometry approach," *IEEE Trans. Veh. Technol.*, vol. 69, no. 4, pp. 3523–3537, Apr. 2020.

[38] S. Mukherjee and J. Lee, "Edge computing-enabled cell-free massive MIMO systems," *IEEE Trans. Wireless Commun.*, vol. 19, no. 4, pp. 2884–2899, Apr. 2020.

[39] A. He, L. Wang, Y. Chen, K.-K. Wong, and M. Elkashlan, "Uplink interference management in massive MIMO enabled heterogeneous cellular networks," *IEEE Wireless Commun. Lett.*, vol. 5, no. 5, pp. 560–563, Oct. 2016.

[40] H. H. Yang, C. Xu, X. Wang, D. Feng, and T. Q. S. Quek, "Understanding age of information in large-scale wireless networks," *IEEE Trans. Wireless Commun.*, vol. 20, no. 5, pp. 3196–3210, May 2021.

[41] E. Björnson and L. Sanguinetti, "Making cell-free massive MIMO competitive with MMSE processing and centralized implementation," *IEEE Trans. Wireless Commun.*, vol. 19, no. 1, pp. 77–90, Jan. 2020.

[42] V. Tripathi, R. Talak, and E. Modiano, "Age of information for discrete time queues," 2019, *arXiv:1901.10463*.

[43] M. Haenggi, "The meta distribution of the SIR in Poisson bipolar and cellular networks," *IEEE Trans. Wireless Commun.*, vol. 15, no. 4, pp. 2577–2589, Apr. 2016.

[44] M. Song, H. H. Yang, H. Shan, J. Lee, and T. Q. S. Quek, "Age of information in wireless networks: Spatiotemporal analysis and locally adaptive power control," *IEEE Trans. Mobile Comput.*, vol. 22, no. 6, pp. 3123–3136, Jun. 2023.

[45] T. Björk, A. Murgoci, and X. Y. Zhou, "Mean–variance portfolio optimization with state-dependent risk aversion," *Math. Finance*, vol. 24, no. 1, pp. 1–24, Jan. 2014.

[46] F. J. Fabozzi, P. N. Kolm, D. A. Pachamanova, and S. Focardi, *Robust Portfolio Optimization and Management*. Hoboken, NJ, USA: Wiley, 2007.

[47] C.-Y. Li et al., "An energy efficiency perspective on rate adaptation for 802.11n NIC," *IEEE Trans. Mobile Comput.*, vol. 15, no. 6, pp. 1333–1347, Jun. 2016.

Meiyan Song received the B.Eng. degree in communication engineering from Wuhan University of Technology, Wuhan, China, in 2018, and the Ph.D. degree in electrical engineering from Zhejiang University, Hangzhou, China, in 2023. She is currently an Associate Professor with the College of Information Engineering, China Jiliang University, Hangzhou. Her research interests include the performance analysis and optimization of wireless networks.

Hangguan Shan (Senior Member, IEEE) received the B.Sc. degree in electrical engineering from Zhejiang University, Hangzhou, China, in 2004, and the Ph.D. degree in electrical engineering from Fudan University, Shanghai, China, in 2009.

From 2009 to 2010, he was a Post-Doctoral Research Fellow with the University of Waterloo, Waterloo, ON, Canada. Since 2011, he has been with the College of Information Science and Electronic Engineering, Zhejiang University, where he is currently an Associate Professor. He is also with Zhejiang Provincial Key Laboratory of Information Processing and Communication Networks, Zhejiang University. His current research interests include machine learning-enabled resource allocation and quality-of-service provisioning in wireless networks. He has co-received the Best Industry Paper Award from the IEEE WCNC'11 and the Best Paper Award from the IEEE WCSP'23 and IEEE/CIC ICCC'24. He has served as a technical program committee member for various international conferences. He is an Associate Editor of the *IET Communications*. He was an Editor of IEEE TRANSACTIONS ON GREEN COMMUNICATIONS AND NETWORKING.

Yu Cheng (Fellow, IEEE) received the B.E. and M.E. degrees in electronic engineering from Tsinghua University, Beijing, China, in 1995 and 1998, respectively, and the Ph.D. degree in electrical and computer engineering from the University of Waterloo, Waterloo, ON, Canada, in 2003. He is currently a Full Professor with the Department of Electrical and Computer Engineering, Illinois Institute of Technology, Chicago, IL, USA. His research interests include wireless network performance analysis, information freshness, machine learning, and network security. He was a recipient of the Best Paper Award at QShine 2007, IEEE ICC 2011, and IEEE/CIC ICCC 2024, the Runner-Up Best Paper Award at ACM MobiHoc 2014, the National Science Foundation (NSF) CAREER Award in 2011, and the IIT Sigma Xi Research Award in 2013. He has served as the several Symposium Co-Chair for IEEE ICC and IEEE GLOBECOM and the Technical Program Committee (TPC) Co-Chair for IEEE/CIC ICCC2015, ICNC 2015, and WASA 2011. He was the Founding Vice Chair of the IEEE ComSoc Technical Subcommittee on Green Communications and Computing. He was an IEEE ComSoc Distinguished Lecturer in 2016 and 2017. He is an Associate Editor of IEEE TRANSACTIONS ON VEHICULAR TECHNOLOGY, IEEE INTERNET OF THINGS JOURNAL, and IEEE WIRELESS COMMUNICATIONS.

Weihua Zhuang (Fellow, IEEE) received the B.Sc. and M.Sc. degrees in electrical engineering from Dalian Maritime University, China, and the Ph.D. degree in electrical engineering from the University of New Brunswick, Canada. Since 1993, she has been a Faculty Member of the Department of Electrical and Computer Engineering, University of Waterloo, Canada, where she is currently an University Professor and an University Research Chair of Wireless Communication Networks. Her current research focuses on network architecture, algorithms and protocols, and service provisioning in future communication systems. She was a recipient of Women's Distinguished Career Award in 2021 from IEEE Vehicular Technology Society, R. A. Fessenden Award in 2021 from IEEE Canada, Award of Merit in 2021 from the Federation of Chinese Canadian Professionals (Ontario), and Technical Recognition Award in Ad Hoc and Sensor Networks in 2017 from IEEE Communications Society. She is a fellow of the Royal Society of Canada (RSC), Canadian Academy of Engineering (CAE), and Engineering Institute of Canada (EIC). She is also the President and an elected member of the Board of Governors (BoG) of the IEEE Vehicular Technology Society. She was the Editor-in-Chief of IEEE TRANSACTIONS ON VEHICULAR TECHNOLOGY (2007–2013), an Editor of IEEE TRANSACTIONS ON WIRELESS COMMUNICATIONS (2005–2009), the General Co-Chair of IEEE/CIC International Conference on Communications in China (ICCC) in 2021, the Technical Program Committee (TPC) Chair/Co-Chair of IEEE Vehicular Technology Conference in Fall 2017 and Fall 2016, the TPC Symposia Chair of the IEEE Globecom 2011, and an IEEE Communications Society Distinguished Lecturer (2008–2011).

Xinyu Li (Member, IEEE) received the Ph.D. degree in industrial engineering from Huazhong University of Science and Technology (HUST), China, in 2009. He is currently a Professor with the Department of Industrial and Manufacturing Systems Engineering, State Key Laboratory of Intelligent Manufacturing Equipment and Technology, School of Mechanical Science and Engineering, HUST. He has published more than 90 refereed articles. His research interests include intelligent algorithm, big data, and machine learning.

Qi Zhang received the B.Sc. degree in computer science from Zhejiang University, Hangzhou, China, in 1999, and the E.M.B.A. degree from Ecole Des Ponts Paris Tech de France in International Business Administration, Shanghai, China, in 2010. He is currently the Executive Vice President of Nokia Shanghai Bell and the Head of Nokia Mobile Network China. He has more than 20 years of experience in internet and telecommunication domain. Since 2002, he has been with Nokia in various technical positions and research and development leadership and business leadership positions. He has been leading the TD-LTE business line since 2013 and has successfully accelerated product roadmap and won business, not only in China but also around world. His research interests include the evolution of mobile communication networks, AI, intelligent throughput efficiency, energy saving, and carbon reduction technologies and solutions in wireless networks. He has been awarded as one of the Top 10 5G industry leaders of China in 2018. He has served as a technical committee member for various national science and technology associates.

Xianhua He received the master's degree in system engineering from Southeast University, Nanjing, China, in 2004. He has over 20 years of experience in internet and telecommunication domain designing wireless communication system products, including PHS, 4G, and 5G. He has held various positions, such as a Software Architect, a Chief Innovation Architect, a System Architect, the Senior Technical Manager, and the Senior Manager of Radio Access Network Architecture and Specification Team. From 2002 to 2005, he was a Senior Software Engineer with UTStarcom Company Ltd. Since 2006, he has been with Nokia, Hangzhou, China, and was recognized as a Distinguished Member of the Technical Staff by Nokia Bell Laboratories in 2020. His research interests include radio resource management, AI, the IoT, energy saving, and V2X solutions in wireless networks.